Science Advances
AAAS

advances.sciencemag.org/cgi/content/full/4/8/eaar8590/DC1

Supplementary Materials for

Acute sleep loss results in tissue-specific alterations in genome-wide DNA methylation state and metabolic fuel utilization in humans

Jonathan Cedernaes*, Milena Schönke, Jakub Orzechowski Westholm, Jia Mi, Alexander Chibalin, Sarah Voisin, Megan Osler, Heike Vogel, Katarina Hörnaeus, Suzanne L. Dickson, Sara Bergström Lind, Jonas Bergquist, Helgi B Schiöth, Juleen R. Zierath, Christian Benedict

*Corresponding author. Email: jonathan.cedernaes@neuro.uu.se

Published 22 August 2018, *Sci. Adv.* **4**, eaar8590 (2018)
DOI: 10.1126/sciadv.aar8590

This PDF file includes:

Supplementary Figures and Figure Legends

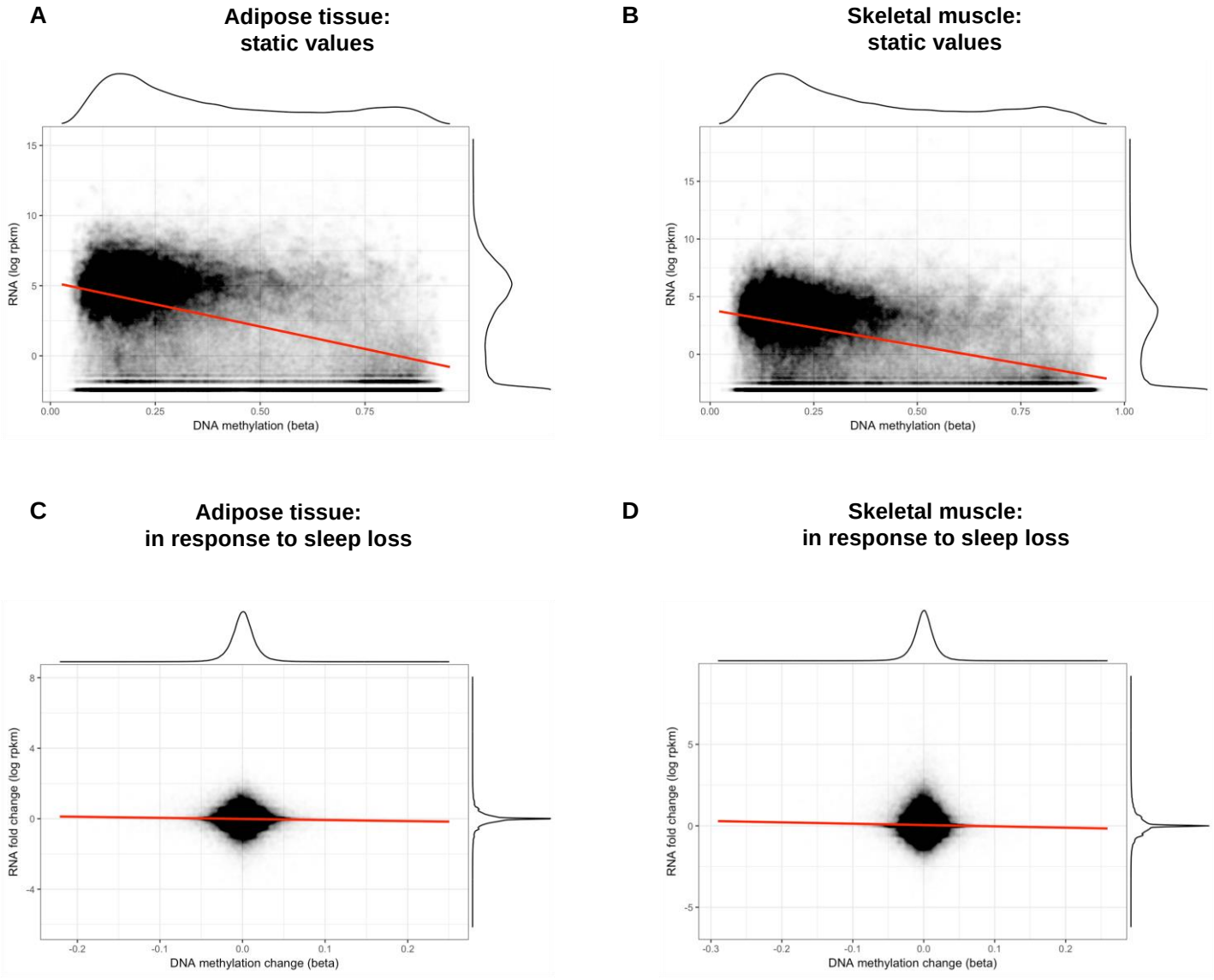

Fig. S1. Correlations between methylation and gene expression levels in subcutaneous adipose tissue and skeletal muscle at baseline and in response to acute sleep loss in humans. Top panels show correlations in "static" samples, i.e. without considering the changes in levels of DNA methylation (shown as beta value on the x axis) and gene expression (shown as log RPKM on the y axis) in response to sleep deprivation, in (**A**) subcutaneous adipose tissue, and (**B**) skeletal muscle. In panels C-D, fold changes in DNA methylation (change in beta level) and gene expression levels (log fold change in RPKM) in response to sleep loss were utilized to analyze correlations between sleep loss-induced changes at these two genomic levels in (**C**) subcutaneous adipose tissue, and (**D**) in skeletal muscle (with n=15 pairs for each analysis).

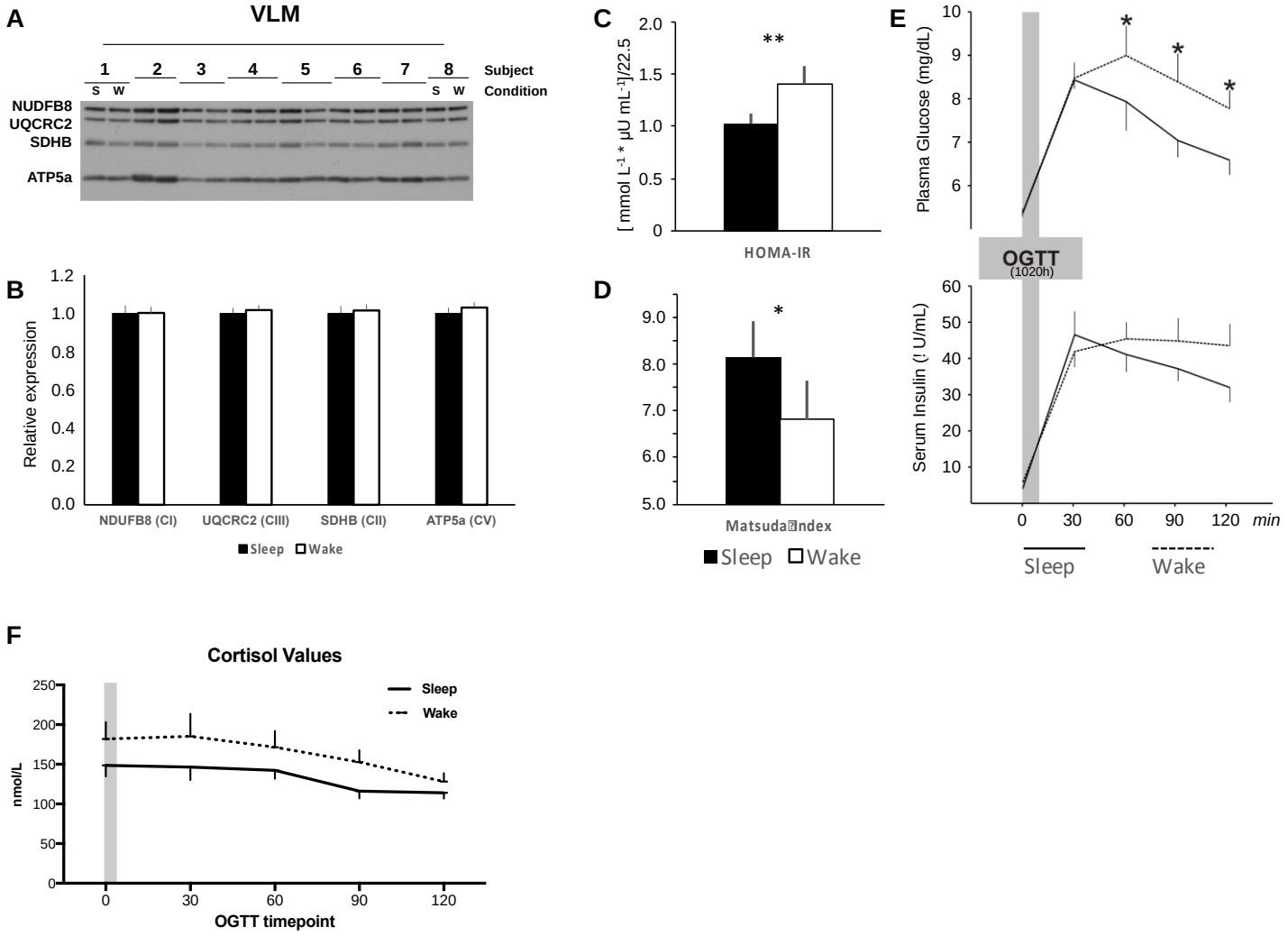

Fig. S2. Insulin sensitivity is adversely affected, and cortisol levels are significantly elevated following acute sleep loss in healthy young men without changes to protein levels of mitochondrial complexes. (**A**) Representative immunoblot and (**B**) quantification of mitochondrial complexes, after normal sleep (s) and sleep loss (*i.e.* overnight wakefulness; "w" / "wake") in vastus lateralis muscle (VLM; showing 8 representative pairs out of a total of 13 analyzed pairs). (**C**) Insulin sensitivity as assessed by HOMA-IR and the (**D**) Matsuda index (*62*) (paired two-sided t-tests), based on post-oral glucose tolerance test (OGTT) (**E**) glucose and insulin values (repeated measures ANOVA effects, glucose: Wake*Time interaction P=0.002, Wake P=0.016, Time P=0.000; insulin: interaction P=0.235, Wake P=0.098, Time P=0.000). (**F**) Serum cortisol analyzed throughout the OGTT (repeated measures ANOVA, see main text; Wake*Time interaction P>0.10). Western blots were normalized to loading control (shown in **Fig. S5D**). Line graphs: sleep, solid lines; sleep loss, dashed lines. Bar graphs: sleep, filled bars; sleep loss, white bars. ATP5a, F(1)F(0) ATP synthase; CI/CII/CIII/CV, mitochondrial complex 1/2/3/5; NUDFB8, NADH:ubiquinone oxidoreductase subunit B8; SDHB, Succinate Dehydrogenase complex iron sulfur subunit B; UQCRC2, Ubiquinol-Cytochrome C Reductase Core Protein II. Values shown as mean ± S.E.M, analysis by ANOVA or two-sided t-tests; ANOVA/biochemical analyses: n=15 pairs. *, P<0.05; **, P<0.01.

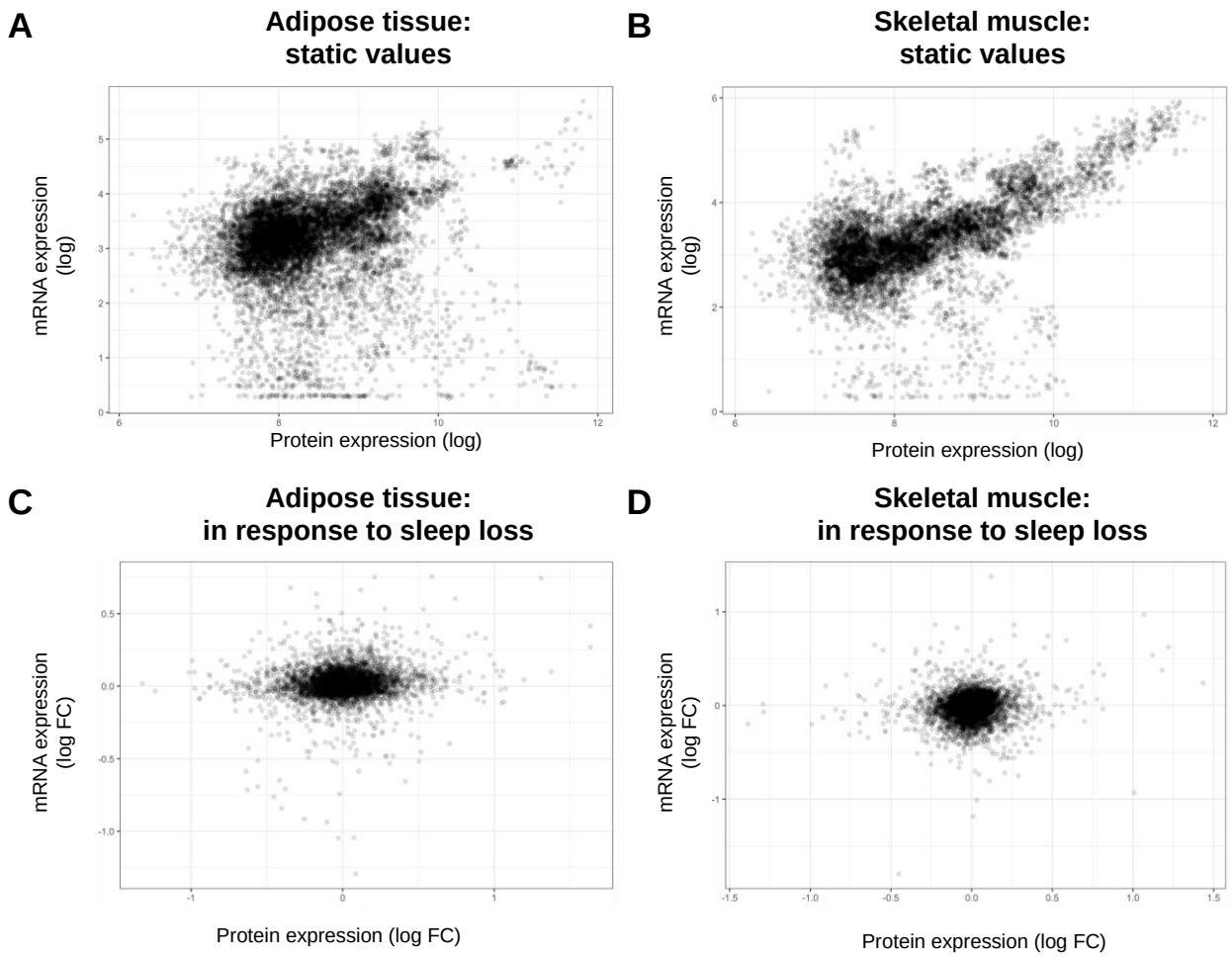
A
Adipose tissue:
static values
mRNA expression
(log)
Protein expression (log)
B
Skeletal muscle:
static values
mRNA expression
(log)
Protein expression (log)
C
Adipose tissue:
in response to sleep loss
mRNA expression
(log FC)
Protein expression (log FC)
D
Skeletal muscle:
in response to sleep loss
mRNA expression
(log FC)
Protein expression (log FC)

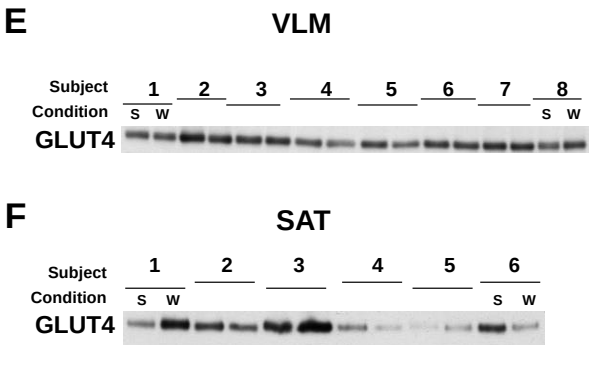
E
VLM
Subject
1 2 3 4 5 6 7 8
Condition
S W S W
GLUT4
F
SAT
Subject
1 2 3 4 5 6
Condition
S W S W
GLUT4

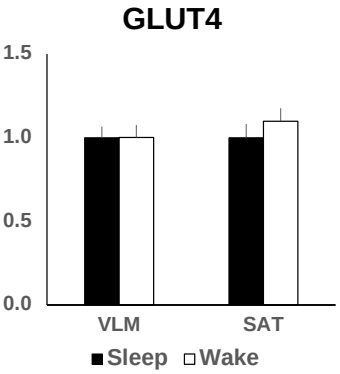
G
GLUT4
1.5
1.0
0.5
0.0
VLM
SAT
Sleep
Wake

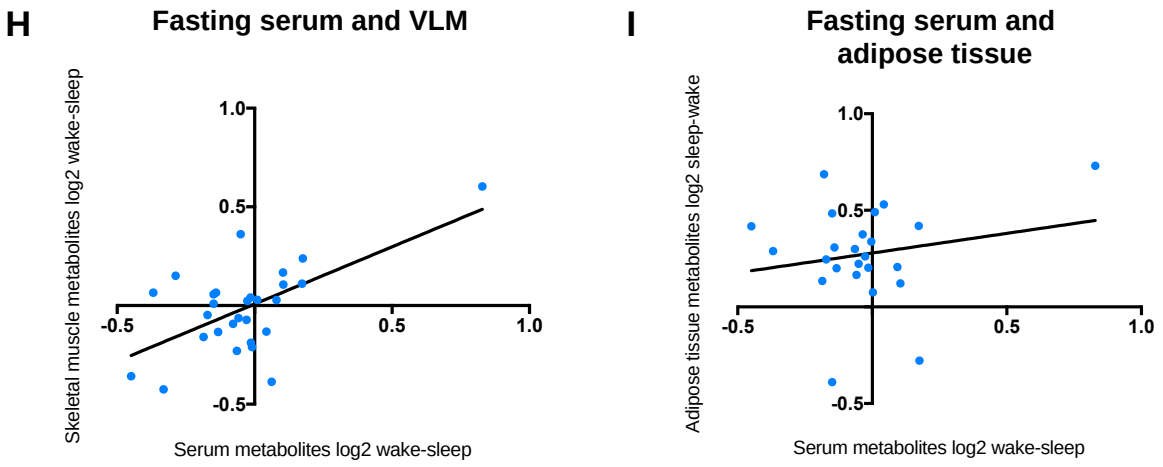
H
Fasting serum and VLM
Skeletal muscle metabolites log2 wake-sleep
Serum metabolites log2 wake-sleep
I
Fasting serum and
adipose tissue
Adipose tissue metabolites log2 sleep-wake
Serum metabolites log2 wake-sleep

Fig. S3. Gene expression and protein levels correlate at baseline but not in response to sleep loss in subcutaneous adipose tissue and skeletal muscle in humans. Top panels show correlations in "static" samples, i.e. without considering the sleep loss-induced changes in levels of mRNA transcripts (from RNA-seq data) or protein levels (identified by mass spectrometry-based proteomic analyses), in (**A**) subcutaneous adipose tissue, and (**B**) skeletal muscle. In panels C-D, fold changes in mRNA transcript and protein levels (following sleep loss compared with sleep) were utilized to analyze correlations between gene expression and protein levels in (**C**) subcutaneous adipose tissue, and (**D**) in skeletal muscle (with n=15 pairs for each analysis) in response to sleep loss. **(E-G)** Immunoblot of GLUT4 in (**E**) *vastus lateralis* muscle (VLM; showing 8 representative pairs; out of 13 analyzed pairs) and (**F**) subcutaneous adipose tissue (SAT; showing 6 representative pairs; out of 11 analyzed pairs) after sleep ("s") and sleep loss ("w"/wake); with quantification of all analyzed pairs in (**G**) (P>0.10 in two-sided t-tests). Values were normalized to loading control (shown in **Fig. S4E-F**). (**H-I**) Changes in metabolite levels (log_2 normalized; sleep loss compared with sleep) were utilized to analyze correlations between sleep loss-induced changes in metabolites identified by gas chromatography coupled to mass spectrometry (GCMS) in (**H**) fasting serum and skeletal muscle (VLM) samples as well as (**I**) between fasting serum and subcutaneous adipose tissue samples in response to acute sleep loss. GLUT4, glucose transporter 4. Values are shown as mean ± S.E.M; protein abundance analyzed using two-sided t-tests.

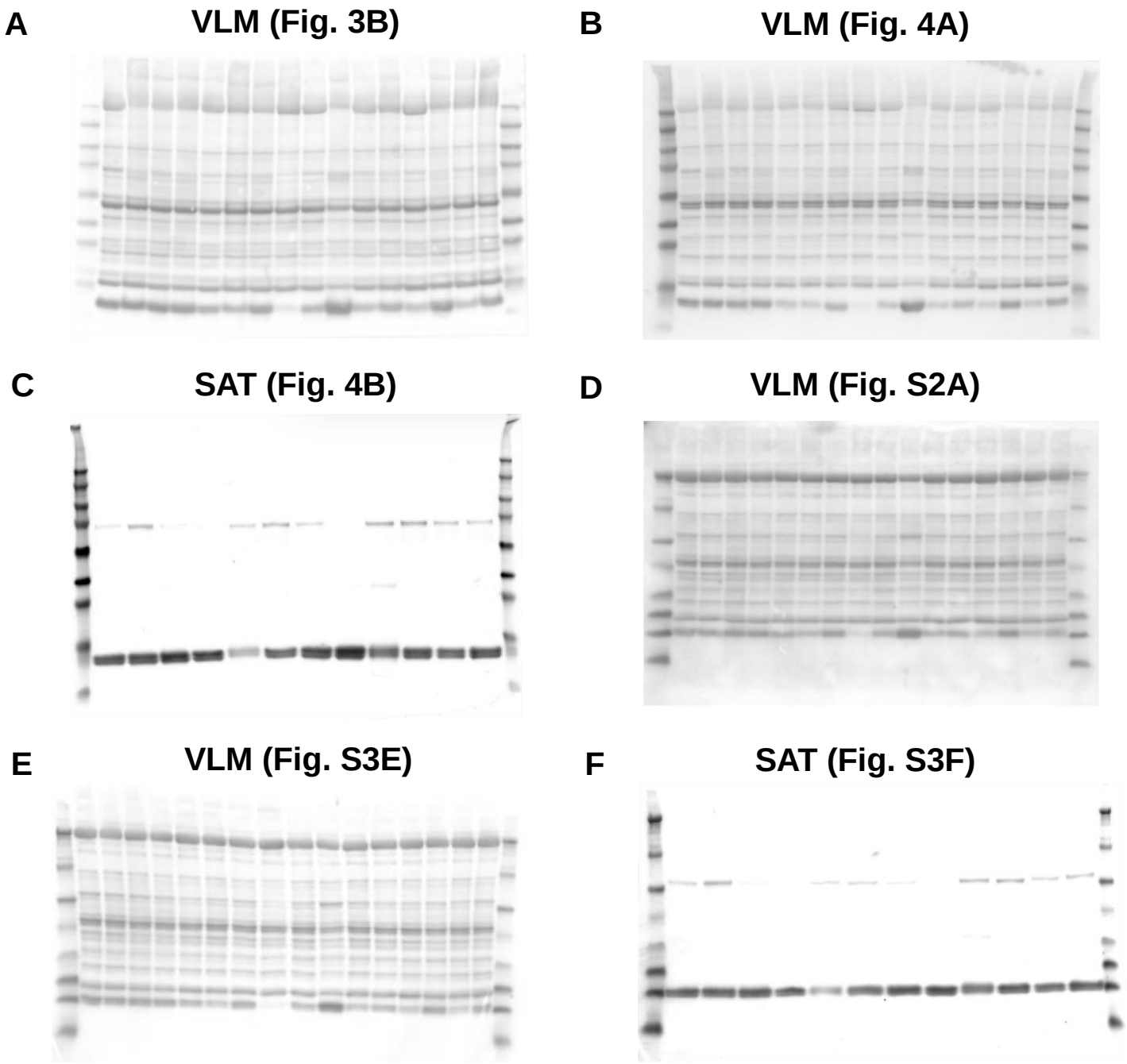

Fig. S4. Loading controls for Western blots used throughout the manuscript. Ponceau staining was used to visually verify protein loading and to quantitatively normalize western blots to total loaded protein content per sample(*61*). Figure shows Ponceau staining for western blots of (**A**) PFK-1 in *vastus lateralis* muscle (VLM) (see **Fig. 3**); BMAL1 in (**B**) VLM and in (**C**) subcutaneous adipose tissue (SAT) (see **Fig. 4**); (**D**) mitochondrial proteins (see **Fig. S2**); and (**E-F**) GLUT4 in VLM and SAT, respectively (see **Fig. S3**). BMAL1, brain and muscle Arnt-like protein-1; GLUT4, glucose transporter 4; PFK-1, phosphofructose kinase 1.

Supplementary Tables

Table S1. Data for the 15 participants that were included in the study. Sleep data refers to the second (intervention) night of the sleep condition. Data shown as mean ± S.E.M. BMI, body mass index; MEQ, morning-eveningness questionnaire; N1, stage 1; N2, stage 2; N3, stage 3 (slow wave sleep), REM, rapid eye movement.

Parameter	Value
Age	22.3 ± 0.5 years
BMI	22.6 ± 0.5 kg/m^2
Waist circumference	82.5 ± 1.8 cm
Hip circumference	98.4 ± 1.1 cm
Waist-hip ratio	0.84 ± 0.01
MEQ score	48.7 ± 2.2
Sleep data:	
• **Total sleep duration**	8.0 h ± 3 min
○ **% of total sleep duration:**	
▪ Awake:	3.8 ± 0.5%
▪ REM sleep:	25 ± 1.2%
▪ N1 sleep:	2.1 ± 0.5%
▪ N2 sleep:	47.7 ± 1.2%
▪ N3 sleep:	21.7 ± 1.5%

Table S2. DMRs and enriched biological pathways based on methylation changes in subcutaneous adipose tissue in response to acute sleep loss. (**A**) Showing hypermethylated and (**B**) *hypo*methylated DMRs, based on mean (Stouffer) FDR-adjusted P-value<0.05, in subcutaneous adipose tissue following sleep loss compared with normal sleep. For each DMR, the following are also listed: minimum FDR value; relation of analyzed DMRs to genes (e.g. near the transcription start site; TSS); chromosome (chr); start and end position; number of probes included in the DMR; width of the DMR; as well as the maximum and mean (absolute) change in beta (methylation) level. (**C**-**E**) Significant DMRs were utilized to identify enriched biological pathways in subcutaneous adipose tissue after sleep loss compared with normal sleep, showing pathways based on (**C**) all (regardless of directionality), (**D**) hypermethylated or (**E**) hypomethylated DMRs in subcutaneous adipose tissue. Listing GO term ID, name of the GO term, the utilized namespace, the total number of genes in each pathway ("N"), the number of annotated genes of a given pathway that were differentially methylated ("DE"), and the FDR-adjusted p value (q value) for the pathway. (**F**) Showing the 20 probes closest to reaching significance (FDR-adjusted) in skeletal muscle in response to sleep loss.

Table S2A. *Hyper*methylated DMRs in subcutaneous adipose tissue after sleep loss compared with sleep.

Chr	Start	End	Width	Nr of probes	Min FDR	Stouffer	Max beta fc	Mean beta fc	Gene TSS	Genomic feature
chr6	32077744	32078624	881	11	2.63E-17	6.17E-05	0.067	0.046	*TNXB*	Near TSS
chr16	8806359	8807043	685	13	1.56E-14	3.99E-04	0.041	0.029	*ABAT*	Near TSS
chr11	73356316	73357741	1426	11	7.88E-16	4.61E-04	0.062	0.033	*PLEKHB1*	Near TSS
chr7	56160409	56161020	612	10	1.19E-10	5.39E-04	0.055	0.045	*PHKG1*	Near TSS
chr10	95516788	95517895	1108	10	6.23E-19	6.77E-04	0.067	0.024	*LGI1*	Near TSS
chr6	106546704	106546824	121	5	2.63E-11	8.97E-04	0.053	0.045	*PRDM1*	Near TSS
chr17	76975944	76976357	414	8	2.11E-11	9.18E-04	0.050	0.036	*LGALS3BP*	Near TSS
chr2	50201413	50201511	99	4	9.20E-12	9.70E-04	0.048	0.043	*NRXN1*	Near TSS
chr8	38385808	38386476	669	6	1.84E-10	1.01E-03	0.062	0.027	*C8orf86*	Near TSS
chr20	19866743	19867145	403	8	7.12E-09	1.20E-03	0.063	0.055	*RIN2*	Near TSS
chr10	56560945	56561543	599	6	2.46E-13	1.70E-03	0.043	0.029	*PCDH15*	Near TSS
chr4	24796689	24797176	488	8	1.06E-09	1.98E-03	0.073	0.047	*SOD3*	Near TSS
chr11	86662968	86663418	451	6	2.11E-09	2.27E-03	0.059	0.049	*FZD4*	Near TSS
chr17	57915665	57915773	109	4	9.21E-10	2.44E-03	0.052	0.042	*VMP1*	Near TSS
chr17	79031091	79031712	622	7	1.01E-09	2.65E-03	0.049	0.034	*BAIAP2*	Near TSS
chr5	35230343	35230935	593	5	1.91E-09	3.07E-03	0.050	0.027	*PRLR*	Near TSS
chr12	91572142	91572276	135	4	1.13E-10	3.12E-03	0.040	0.037	*DCN*	Near TSS
chr22	31002892	31003587	696	9	1.10E-11	3.43E-03	0.023	0.011	*PES1*	Near TSS

chr12	8834114	8834151	38	3	3.12E-10	3.48E-03	0.056	0.047	*RIMKLB*	Near TSS
chr12	25801455	25801621	167	4	3.17E-08	3.70E-03	0.063	0.057	*IFLTD1*	Near TSS
chr17	7791630	7792674	1045	8	7.60E-12	3.80E-03	0.044	0.025	*CHD3*	Near TSS
chr7	114055074	114055210	137	6	3.23E-08	3.82E-03	0.055	0.048	*FOXP2*	Near TSS
chr10	130830829	130831421	593	8	5.79E-10	3.95E-03	0.047	0.030		Intergenic region
chr4	154125208	154125720	513	9	9.56E-12	3.95E-03	0.067	0.041	*TRIM2*	Near TSS
chr1	103573700	103574958	1259	10	3.41E-16	3.98E-03	0.043	0.017	*COL11A1*	Near TSS
chr10	5227162	5227757	596	3	4.22E-10	4.03E-03	0.067	0.049	*AKR1CL1*	Near TSS
chr3	194090132	194090730	599	6	5.40E-11	4.27E-03	0.035	0.012	*LRRC15*	Near TSS
chr8	39171620	39172120	501	9	1.68E-11	4.71E-03	0.040	0.025	*ADAM5*	Near TSS
chr17	42247565	42248358	794	8	1.18E-13	5.27E-03	0.047	0.027	*ASB16*	Near TSS
chr11	122073211	122074433	1223	9	5.51E-16	5.52E-03	0.045	0.023	*RP11-820L6.1*	Near TSS
chr7	157462914	157463355	442	3	1.47E-10	5.55E-03	0.063	0.049		Intron
chr1	165512980	165513716	737	8	4.18E-13	5.69E-03	0.036	0.018	*LRRC52*	Near TSS
chr4	111557894	111558224	331	3	1.01E-09	5.82E-03	0.019	0.014	*PITX2*	Near TSS
chr13	36944294	36944649	356	8	3.15E-11	5.91E-03	0.037	0.026	*SPG20*	Near TSS
chr11	61716821	61717334	514	6	7.40E-11	5.96E-03	0.030	0.019	*BEST1*	Near TSS
chr7	87936225	87936923	699	7	4.90E-10	6.63E-03	0.041	0.014	*STEAP4*	Near TSS
chr3	196242197	196242423	227	3	1.38E-08	6.77E-03	0.049	0.000	*SMCO1*	Near TSS
chr16	86376985	86377053	69	2	4.45E-11	7.14E-03	0.033	0.030	*LINC00917*	Near TSS
chr6	27182908	27182976	69	3	4.65E-08	7.19E-03	0.031	0.024	*RP11-209A2.1*	Near TSS
chr2	108904812	108905468	657	4	7.02E-13	7.34E-03	0.054	0.036	*SULT1C2*	Near TSS
chr3	122712138	122712271	134	3	3.67E-08	7.36E-03	0.041	0.036	*SEMA5B*	Near TSS
chr6	133188277	133188565	289	3	3.01E-10	7.61E-03	0.038	0.035	*HMGB1P13*	Near TSS
chr7	80267619	80267943	325	2	4.30E-11	7.77E-03	0.074	0.069	*CD36*	Near TSS
chr12	47219626	47220092	467	12	1.29E-10	7.89E-03	0.034	0.022	*SLC38A4*	Near TSS
chr7	28338584	28338985	402	6	8.89E-09	8.49E-03	0.037	0.017	*CREB5*	Near TSS
chr13	31506324	31507139	816	10	1.60E-11	8.69E-03	0.048	0.029	*TEX26-AS1*	Near TSS
chr1	156459986	156460747	762	5	4.07E-11	9.25E-03	0.023	0.012	*MEF2D*	Near TSS
chr5	148442554	148442890	337	5	1.81E-08	9.29E-03	0.051	0.029	*CTC-529P8.1*	Near TSS
chr7	21209165	21209509	345	3	1.62E-08	9.73E-03	0.038	0.022		Intergenic region
chr13	45492329	45492839	511	4	2.79E-09	9.99E-03	0.011	0.009		Intergenic region
chr1	156251280	156251456	177	3	1.89E-10	1.12E-02	0.036	0.031	*SMG5*	Near TSS

chr3	165555103	165555160	58	2	2.37E-08	1.40E-02	0.063	0.045	*BCHE*	Near TSS
chr10	93334974	93335196	223	4	2.73E-08	1.50E-02	0.051	0.037		Intergenic region
chr5	150019496	150019603	108	2	1.14E-10	1.52E-02	0.040	0.039	*SYNPO*	Near TSS
chr11	41481358	41481655	298	5	9.06E-09	1.54E-02	0.022	0.014	*LRRC4C*	Near TSS
chrX	66763009	66765122	2114	19	6.98E-14	1.55E-02	0.048	0.014	*AR*	Near TSS
chr1	47656423	47656853	431	2	1.70E-08	1.59E-02	0.024	0.007	*PDZK1IP1*	Near TSS
chr3	112012867	112013646	780	6	2.94E-10	1.63E-02	-0.045	0.017	*SLC9C1*	Near TSS
chr10	104535792	104536695	904	10	6.86E-10	1.66E-02	0.040	0.017	*WBP1L*	Near TSS
chr14	67982430	67982456	27	2	3.51E-09	1.66E-02	0.033	0.031	*TMEM229B*	Near TSS
chrX	67867130	67867448	319	8	3.44E-08	1.67E-02	0.076	0.040	*STARD8*	Near TSS
chr2	219472218	219472410	193	2	2.26E-08	1.74E-02	0.059	0.054	*PLCD4*	Near TSS
chr16	66995143	66995461	319	3	3.02E-08	1.74E-02	0.042	0.022	*CES3*	Near TSS
chr9	116062223	116062240	18	2	9.12E-09	1.74E-02	0.054	0.046	*RNF183*	Near TSS
chr6	31734147	31734580	434	10	3.66E-09	1.74E-02	0.041	0.031	*SAPCD1-AS1*	Near TSS
chr6	30653167	30653799	633	12	2.83E-10	1.82E-02	0.033	0.018	*PPP1R18*	Near TSS
chr6	32026299	32026891	593	9	6.90E-10	1.88E-02	0.036	0.023		Intron
chr11	76432800	76433300	501	12	7.71E-15	1.98E-02	0.028	0.010	*RP11-672A2.1*	Near TSS
chr8	49832881	49833279	399	2	1.29E-10	2.06E-02	0.051	0.045	*SNAI2*	Near TSS
chr1	151137619	151138516	898	11	9.22E-11	2.18E-02	0.033	0.013	*SCNM1*	Near TSS
chr6	130182053	130182620	568	7	4.78E-09	2.22E-02	0.053	0.024	*TMEM244*	Near TSS
chr6	33157222	33157811	590	4	3.15E-11	2.31E-02	0.047	0.031	*COL11A2*	Near TSS
chr19	45409440	45409713	274	2	1.02E-08	2.35E-02	0.021	0.016	*APOE*	Near TSS
chr12	54411193	54411473	281	3	2.70E-10	2.45E-02	0.018	0.013	*RP11-834C11.14*	Near TSS
chr12	128866172	128866735	564	6	5.89E-11	2.47E-02	0.042	0.027		Intron
chr12	4488749	4489221	473	6	1.23E-11	2.53E-02	0.040	0.010	*FGF23*	Near TSS
chr15	64673455	64673618	164	3	5.23E-08	2.56E-02	0.017	0.015	*KIAA0101*	Near TSS
chr3	112359935	112360446	512	2	6.56E-10	2.63E-02	0.043	0.034	*CCDC80*	Near TSS
chr7	88425077	88425148	72	5	4.80E-08	2.67E-02	0.036	0.025	*C7orf62*	Near TSS
chr7	27140942	27141139	198	4	3.36E-08	2.91E-02	0.058	0.044	*HOXA2*	Near TSS
chr1	2448477	2448495	19	2	2.91E-08	3.06E-02	0.009	0.008	*PANK4*	Near TSS
chr15	32162783	32163262	480	8	1.29E-10	3.08E-02	-0.040	0.003	*OTUD7A*	Near TSS
chr19	35606534	35606554	21	2	3.82E-08	3.10E-02	0.046	0.040	*FXYD3*	Near TSS
chr22	31536431	31536585	155	5	7.02E-09	3.19E-02	0.033	0.023	*PLA2G3*	Near TSS

chr12	16757954	16758836	883	10	3.94E-15	3.70E-02	0.022	0.012	*LMO3*	Near TSS
chr6	32086425	32087190	766	13	1.62E-14	3.71E-02	0.037	0.017	*ATF6B*	Near TSS
chrX	85302489	85302864	376	5	6.27E-10	4.45E-02	0.056	0.020	*CHM*	Near TSS
chr4	3371520	3372206	687	7	8.47E-09	4.52E-02	0.048	0.026	*RGS12*	Near TSS
chr12	88536400	88536575	176	5	9.05E-13	4.52E-02	0.077	0.020	*TMTC3*	Near TSS
chr1	40723164	40723194	31	2	8.23E-09	4.62E-02	0.021	0.016	*RP1-39G22.7*	Near TSS
chr11	8832817	8833095	279	6	3.67E-10	4.71E-02	0.048	0.024	*ST5*	Near TSS
chr6	30657882	30658612	731	8	6.81E-11	4.77E-02	0.032	0.013	*NRM*	Near TSS

Table S2B. *Hypo*methylated DMRs in subcutaneous adipose tissue after sleep loss compared with sleep.

Chr	Start	End	Width	Nr of probes	Min FDR	Stouffer	Max beta fc	Mean beta fc	Gene TSS	Genomic feature
chr11	2321770	2323272	1503	29	1.51E-14	7.35E-05	-0.058	-0.042	*TSPAN32*	Near TSS
chr15	96886805	96888024	1220	11	4.73E-13	3.62E-04	-0.045	-0.030		Immediate downstream
chr20	3065343	3066014	672	8	3.22E-11	6.71E-04	-0.056	-0.037	*AVP*	Near TSS
chr10	49892741	49893549	809	15	6.31E-11	8.25E-04	-0.054	-0.040	*WDFY4*	Near TSS
chr19	46521467	46522575	1109	8	6.79E-13	1.77E-03	-0.023	-0.014	*CCDC61*	Near TSS
chr15	25447222	25447799	578	3	4.29E-11	2.53E-03	-0.026	-0.023	*SNORD115-18*	Near TSS
chr12	54784747	54785320	574	8	6.98E-10	3.30E-03	-0.074	-0.035	*ZNF385A*	Near TSS
chr12	131589169	131589455	287	5	2.89E-09	3.53E-03	-0.017	0.000		Exon
chr10	134024191	134024476	286	3	2.50E-11	4.41E-03	-0.017	-0.014		Immediate downstream
chr8	144408506	144408955	450	5	2.13E-08	4.77E-03	-0.049	-0.029	*TOP1MT*	Near TSS
chr1	64669125	64669599	475	9	1.46E-11	5.56E-03	-0.026	-0.015	*UBE2U*	Near TSS
chr18	19756877	19757468	592	4	1.63E-09	5.99E-03	-0.052	-0.039	*RP11-627G18.2*	Near TSS
chr20	57463900	57464571	672	9	7.12E-09	6.89E-03	-0.026	-0.018	*GNAS*	Near TSS
chr6	116447667	116448231	565	2	2.22E-11	7.19E-03	-0.034	-0.029	*COL10A1*	Near TSS
chr22	24822802	24823554	753	10	5.43E-12	7.42E-03	-0.060	-0.032	*ADORA2A*	Near TSS
chr7	1267987	1268188	202	2	1.88E-11	8.37E-03	-0.061	-0.058	*UNCX*	Near TSS
chr4	4864110	4864902	793	12	6.24E-10	9.27E-03	-0.050	-0.028	*MSX1*	Near TSS
chr16	87511403	87511500	98	2	2.25E-08	1.03E-02	-0.055	-0.039		Intron
chr5	666524	666707	184	2	3.10E-08	1.04E-02	-0.021	-0.017	*AC026740.1*	Near TSS

chr7	2128263	2128505	243	2	2.29E-08	1.07E-02	-0.025	-0.023	*MAD1L1*	Near TSS
chr3	12858887	12858926	40	2	3.98E-08	1.10E-02	-0.041	-0.038		Exon
chr11	68611016	68611328	313	3	1.20E-08	1.18E-02	-0.036	-0.025	*CPT1A*	Near TSS
chr11	66822853	66822904	52	2	2.58E-10	1.18E-02	-0.025	-0.022	*RHOD*	Near TSS
chr6	31760426	31761076	651	12	2.01E-09	1.18E-02	-0.036	-0.018	*VARS*	Near TSS
chr11	45721162	45721257	96	2	1.55E-09	1.22E-02	-0.027	-0.023		Intergenic region
chr16	56388908	56389029	122	3	3.16E-09	1.34E-02	-0.025	-0.023	*RP11-441F2.5*	Near TSS
chr13	45993412	45993749	338	2	1.54E-10	1.40E-02	-0.028	-0.022	*SLC25A30*	Near TSS
chr20	36157577	36157764	188	5	8.54E-09	1.42E-02	-0.021	-0.017	*PPIAP3*	Near TSS
chr18	9885797	9885809	13	2	2.81E-08	1.44E-02	-0.015	-0.014	*TXNDC2*	Near TSS
chrX	21874093	21874808	716	6	2.38E-11	1.49E-02	-0.026	-0.018	*YY2*	Near TSS
chr2	177027075	177028162	1088	8	7.67E-09	1.65E-02	-0.050	-0.035	*HOXD3*	Near TSS
chr4	3416849	3416881	33	2	1.97E-10	1.78E-02	-0.059	-0.052	*RGS12*	Near TSS
chr6	30297174	30297941	768	12	5.78E-10	1.81E-02	-0.052	-0.036	*TRIM39*	Near TSS
chr13	114888999	114889227	229	3	3.95E-09	1.82E-02	-0.025	-0.018		Intron
chr17	38658717	38659139	423	3	8.13E-12	2.06E-02	-0.023	-0.012	*TNS4*	Near TSS
chr15	28051072	28051262	191	2	2.19E-09	2.18E-02	-0.022	-0.018		Intron
chr17	76128906	76129533	628	5	1.51E-10	2.25E-02	-0.045	-0.024	*TMC6*	Near TSS
chr6	35704822	35704928	107	2	1.00E-09	2.38E-02	-0.023	-0.018	*ARMC12*	Near TSS
chr4	186944909	186945339	431	5	1.53E-09	2.51E-02	-0.032	-0.012	*RNU4-64P*	Near TSS
chr1	231155449	231156359	911	13	1.04E-09	2.54E-02	0.053	-0.003	*MIR1182*	Near TSS
chr9	133885009	133885058	50	2	9.23E-09	2.59E-02	-0.026	0.000	*LAMC3*	Near TSS
chr6	30552010	30552133	124	4	1.16E-08	2.61E-02	-0.021	-0.008	*MIR877*	Near TSS
chr16	129454	129562	109	2	2.63E-08	2.61E-02	-0.036	-0.030	*MPG*	Near TSS
chr4	7436199	7436259	61	2	2.18E-09	2.64E-02	-0.023	-0.019	*PSAPL1*	Near TSS
chr6	32062914	32065211	2298	57	9.76E-17	2.71E-02	-0.030	-0.013		Immediate downstream
chr5	1501109	1501670	562	3	4.77E-12	2.84E-02	-0.023	-0.016		Exon
chr10	131567498	131567534	37	2	3.98E-08	2.94E-02	-0.038	-0.028	*RP11-109A6.3*	Near TSS
chr4	68928981	68929413	433	4	4.79E-11	2.99E-02	-0.042	-0.018	*SYT14L*	Near TSS
chr12	115133735	115134496	762	8	5.31E-09	3.49E-02	-0.036	-0.031		Intergenic region
chr17	1961440	1961778	339	3	1.36E-08	3.64E-02	-0.026	-0.022	*HIC1*	Near TSS
chr1	92952897	92953279	383	4	3.16E-09	3.82E-02	-0.075	-0.040	*GFI1*	Near TSS

chr4	4860190	4860698	509	10	3.92E-09	3.92E-02	-0.038	-0.026	*MSX1*	Near TSS
chr20	57582894	57583188	295	8	2.53E-08	4.25E-02	-0.071	-0.042	*CTSZ*	Near TSS
chr11	2183505	2183864	360	5	1.59E-08	4.44E-02	-0.024	-0.015	*INS*	Near TSS
chr5	93905343	93905482	140	4	2.32E-08	4.61E-02	-0.022	-0.016	*RP11-461G12.2*	Near TSS
chr12	131493585	131493891	307	2	5.35E-10	4.86E-02	-0.023	-0.015		Immediate downstream

Table S2C. Enriched biological pathways based on *all* (hyper- and hypomethylated) significant DMRs in subcutaneous adipose tissue after sleep loss compared with sleep.

GO term ID	Term name	Namespace	N	DE	q value
GO:0061448	connective tissue development	BP	235	10	0.0000003
GO:0051216	cartilage development	BP	180	9	0.0000003
GO:0050877	nervous system process	BP	1217	21	0.0000006
GO:0023051	regulation of signaling	BP	3363	36	0.0000043
GO:0050806	positive regulation of synaptic trans…	BP	134	7	0.0000051
GO:0001501	skeletal system development	BP	486	12	0.0000061
GO:0010646	regulation of cell communication	BP	3314	35	0.0000085
GO:0003008	system process	BP	1953	25	0.0000102
GO:0022610	biological adhesion	BP	1339	20	0.0000104
GO:0043516	regulation of DNA damage response, si…	BP	30	4	0.0000149
GO:0050804	modulation of chemical synaptic trans…	BP	306	9	0.0000243
GO:0009653	anatomical structure morphogenesis	BP	2470	28	0.0000258
GO:0007610	behavior	BP	572	12	0.0000307
GO:0007155	cell adhesion	BP	1332	19	0.0000335
GO:0043517	positive regulation of DNA damage res…	BP	14	3	0.000043
GO:0030154	cell differentiation	BP	3908	37	0.0000508
GO:0051957	positive regulation of amino acid tra…	BP	15	3	0.0000535
GO:1903793	positive regulation of anion transpor…	BP	42	4	0.000058
GO:0050890	cognition	BP	270	8	0.0000663
GO:0007267	cell-cell signaling	BP	1561	20	0.0000911
GO:0048705	skeletal system morphogenesis	BP	210	7	0.0000927
GO:0035556	intracellular signal transduction	BP	2659	28	0.0000962
GO:0048856	anatomical structure development	BP	5518	46	0.0001021

GO:0009887	animal organ morphogenesis	BP	985	15	0.0001208
GO:0048869	cellular developmental process	BP	4078	37	0.0001274
GO:0042359	vitamin D metabolic process	BP	20	3	0.0001316
GO:0032502	developmental process	BP	5921	48	0.0001333
GO:0046942	carboxylic acid transport	BP	303	8	0.0001472
GO:0010647	positive regulation of cell communica…	BP	1619	20	0.0001493
GO:1901798	positive regulation of signal transdu…	BP	21	3	0.000153
GO:0033993	response to lipid	BP	893	14	0.0001532
GO:0009966	regulation of signal transduction	BP	3031	30	0.000156
GO:0023056	positive regulation of signaling	BP	1625	20	0.0001569
GO:0050896	response to stimulus	BP	8322	61	0.0001608
GO:0032989	cellular component morphogenesis	BP	1018	15	0.0001731
GO:0015849	organic acid transport	BP	311	8	0.0001759
GO:0010894	negative regulation of steroid biosyn…	BP	22	3	0.0001765
GO:1901700	response to oxygen-containing compoun…	BP	1512	19	0.0001797
GO:0045600	positive regulation of fat cell diffe…	BP	56	4	0.0001802
GO:0006820	anion transport	BP	587	11	0.0001804
GO:0044070	regulation of anion transport	BP	105	5	0.0001882
GO:0023052	signaling	BP	6178	49	0.0001902
GO:0045595	regulation of cell differentiation	BP	1649	20	0.0001908
GO:0010648	negative regulation of cell communica…	BP	1274	17	0.0002032
GO:0000902	cell morphogenesis	BP	921	14	0.0002107
GO:0023057	negative regulation of signaling	BP	1278	17	0.0002109
GO:0050866	negative regulation of cell activatio…	BP	169	6	0.0002124
GO:0045939	negative regulation of steroid metabo…	BP	24	3	0.0002303
GO:0048468	cell development	BP	1944	22	0.0002342
GO:0015909	long-chain fatty acid transport	BP	62	4	0.0002675
GO:0007275	multicellular organism development	BP	5056	42	0.0002721
GO:0001958	endochondral ossification	BP	26	3	0.0002937
GO:0036075	replacement ossification	BP	26	3	0.0002937
GO:0060348	bone development	BP	183	6	0.0003257
GO:0048585	negative regulation of response to st…	BP	1458	18	0.0003361
GO:0050795	regulation of behavior	BP	66	4	0.0003403

GO:0051955	regulation of amino acid transport	BP	28	3	0.0003673
GO:0022008	neurogenesis	BP	1472	18	0.000377
GO:0035116	embryonic hindlimb morphogenesis	BP	29	3	0.0004082
GO:0032892	positive regulation of organic acid t…	BP	29	3	0.0004082
GO:0032501	multicellular organismal process	BP	7084	53	0.0004088
GO:0009967	positive regulation of signal transdu…	BP	1483	18	0.0004121
GO:0007626	locomotory behavior	BP	192	6	0.0004206
GO:0007154	cell communication	BP	6196	48	0.0004223
GO:0015711	organic anion transport	BP	449	9	0.0004391
GO:0032102	negative regulation of response to ex…	BP	272	7	0.00045
GO:0019216	regulation of lipid metabolic process	BP	358	8	0.000452
GO:0000904	cell morphogenesis involved in differ…	BP	658	11	0.0004759
GO:1902531	regulation of intracellular signal tr…	BP	1772	20	0.0004869
GO:0051954	positive regulation of amine transpor…	BP	31	3	0.0004985
GO:0030182	neuron differentiation	BP	1250	16	0.0005025
GO:0048699	generation of neurons	BP	1378	17	0.0005042
GO:0007399	nervous system development	BP	2211	23	0.000553
GO:0009605	response to external stimulus	BP	2071	22	0.000562
GO:0050793	regulation of developmental process	BP	2360	24	0.0005686
GO:0050953	sensory perception of light stimulus	BP	206	6	0.0006096
GO:0045833	negative regulation of lipid metaboli…	BP	78	4	0.0006432
GO:2001233	regulation of apoptotic signaling pat…	BP	378	8	0.0006457
GO:0016049	cell growth	BP	474	9	0.0006474
GO:0050878	regulation of body fluid levels	BP	480	9	0.0007078
GO:0009968	negative regulation of signal transdu…	BP	1169	15	0.0007434
GO:0046879	hormone secretion	BP	298	7	0.000772
GO:0007605	sensory perception of sound	BP	143	5	0.0007783
GO:0035137	hindlimb morphogenesis	BP	37	3	0.0008431
GO:0040007	growth	BP	937	13	0.0008434
GO:0051716	cellular response to stimulus	BP	6947	51	0.0009454
GO:0051341	regulation of oxidoreductase activity	BP	87	4	0.0009696
GO:0009914	hormone transport	BP	310	7	0.0009718
GO:1902532	negative regulation of intracellular …	BP	503	9	0.000984

GO:0060349	bone morphogenesis	BP	88	4	0.0010119
GO:0015718	monocarboxylic acid transport	BP	153	5	0.0010538
GO:0008150	biological_process	BP	16519	97	0.001054
GO:0015908	fatty acid transport	BP	90	4	0.0011003
GO:0033273	response to vitamin	BP	90	4	0.0011003
GO:0048167	regulation of synaptic plasticity	BP	155	5	0.0011166
GO:0055081	anion homeostasis	BP	41	3	0.00114
GO:0007611	learning or memory	BP	233	6	0.0011547
GO:0009888	tissue development	BP	1901	20	0.00117
GO:0022414	reproductive process	BP	1356	16	0.0011958
GO:0000003	reproduction	BP	1357	16	0.001205
GO:0023061	signal release	BP	417	8	0.0012148
GO:0006775	fat-soluble vitamin metabolic process	BP	42	3	0.0012232
GO:0098869	cellular oxidant detoxification	BP	93	4	0.0012429
GO:0051094	positive regulation of developmental …	BP	1233	15	0.0012712
GO:0050954	sensory perception of mechanical stim…	BP	160	5	0.0012857
GO:0048732	gland development	BP	421	8	0.0012906
GO:0030199	collagen fibril organization	BP	43	3	0.0013102
GO:0033574	response to testosterone	BP	43	3	0.0013102
GO:0007599	hemostasis	BP	328	7	0.0013455
GO:0030198	extracellular matrix organization	BP	329	7	0.0013691
GO:0043062	extracellular structure organization	BP	330	7	0.0013931
GO:0050905	neuromuscular process	BP	96	4	0.001398
GO:0051353	positive regulation of oxidoreductase…	BP	44	3	0.0014009
GO:1990748	cellular detoxification	BP	97	4	0.0014525
GO:0007600	sensory perception	BP	873	12	0.0014538
GO:0046890	regulation of lipid biosynthetic proc…	BP	166	5	0.0015128
GO:1901701	cellular response to oxygen-containin…	BP	1005	13	0.0015869
GO:0045597	positive regulation of cell different…	BP	884	12	0.0016152
GO:0098754	detoxification	BP	101	4	0.0016856
GO:0035094	response to nicotine	BP	47	3	0.0016966
GO:0046883	regulation of hormone secretion	BP	252	6	0.0017205
GO:0007165	signal transduction	BP	5695	43	0.0018018

GO:0051055	negative regulation of lipid biosynth…	BP	48	3	0.0018031
GO:1901796	regulation of signal transduction by …	BP	175	5	0.0019071
GO:0048731	system development	BP	4505	36	0.0019117
GO:0032890	regulation of organic acid transport	BP	49	3	0.0019138
GO:0048522	positive regulation of cellular proce…	BP	4846	38	0.0019245
GO:0097237	cellular response to toxic substance	BP	105	4	0.0019435
GO:0098609	cell-cell adhesion	BP	784	11	0.0019598
GO:0071396	cellular response to lipid	BP	558	9	0.0020083
GO:0060350	endochondral bone morphogenesis	BP	50	3	0.0020285
GO:0060425	lung morphogenesis	BP	50	3	0.0020285
GO:0046426	negative regulation of JAK-STAT casca…	BP	50	3	0.0020285
GO:1904893	negative regulation of STAT cascade	BP	50	3	0.0020285
GO:0030330	DNA damage response, signal transduct…	BP	109	4	0.0022275
GO:0019935	cyclic-nucleotide-mediated signaling	BP	112	4	0.0024584
GO:0070527	platelet aggregation	BP	54	3	0.0025301
GO:0032768	regulation of monooxygenase activity	BP	54	3	0.0025301
GO:0099565	chemical synaptic transmission, posts…	BP	114	4	0.0026212
GO:0034381	plasma lipoprotein particle clearance	BP	55	3	0.0026664
GO:0046717	acid secretion	BP	115	4	0.0027053
GO:0097190	apoptotic signaling pathway	BP	584	9	0.0027252
GO:1905114	cell surface receptor signaling pathw…	BP	585	9	0.0027563
GO:0045598	regulation of fat cell differentiatio…	BP	116	4	0.0027912
GO:0048812	neuron projection morphogenesis	BP	587	9	0.0028195
GO:0010033	response to organic substance	BP	2965	26	0.0028457
GO:0001763	morphogenesis of a branching structur…	BP	193	5	0.0029142
GO:0010817	regulation of hormone levels	BP	481	8	0.0029528
GO:0032101	regulation of response to external st…	BP	707	10	0.0029647
GO:0001558	regulation of cell growth	BP	380	7	0.0030769
GO:0032963	collagen metabolic process	BP	120	4	0.0031537
GO:0006725	cellular aromatic compound metabolic …	BP	5857	43	0.0031915
GO:0048706	embryonic skeletal system development	BP	121	4	0.0032491
GO:0098916	anterograde trans-synaptic signaling	BP	600	9	0.0032587
GO:0007268	chemical synaptic transmission	BP	600	9	0.0032587

GO:0120039	plasma membrane bounded cell projecti…	BP	601	9	0.0032946
GO:0099536	synaptic signaling	BP	602	9	0.0033308
GO:0099537	trans-synaptic signaling	BP	602	9	0.0033308
GO:0048858	cell projection morphogenesis	BP	604	9	0.0034042
GO:0097755	positive regulation of blood vessel d…	BP	60	3	0.0034154
GO:0045834	positive regulation of lipid metaboli…	BP	123	4	0.0034457
GO:0042770	signal transduction in response to DN…	BP	123	4	0.0034457
GO:0034654	nucleobase-containing compound biosyn…	BP	4151	33	0.0034632
GO:0090304	nucleic acid metabolic process	BP	5008	38	0.0035241
GO:0007601	visual perception	BP	202	5	0.003541
GO:0009581	detection of external stimulus	BP	124	4	0.003547
GO:1901360	organic cyclic compound metabolic pro…	BP	6069	44	0.003574
GO:0044259	multicellular organismal macromolecul…	BP	125	4	0.0036503
GO:0022603	regulation of anatomical structure mo…	BP	982	12	0.0038164
GO:0008152	metabolic process	BP	11048	70	0.0038423
GO:0009582	detection of abiotic stimulus	BP	127	4	0.003863
GO:0010977	negative regulation of neuron project…	BP	127	4	0.003863
GO:0045444	fat cell differentiation	BP	207	5	0.0039283
GO:0046903	secretion	BP	1528	16	0.0039736
GO:0008015	blood circulation	BP	506	8	0.0040085
GO:0016042	lipid catabolic process	BP	299	6	0.0040124
GO:1901362	organic cyclic compound biosynthetic …	BP	4358	34	0.0040128
GO:0048583	regulation of response to stimulus	BP	3858	31	0.004066
GO:2001234	negative regulation of apoptotic sign…	BP	209	5	0.0040914
GO:0046889	positive regulation of lipid biosynth…	BP	64	3	0.0040986
GO:0051881	regulation of mitochondrial membrane …	BP	64	3	0.0040986
GO:0032990	cell part morphogenesis	BP	623	9	0.0041666
GO:0097746	regulation of blood vessel diameter	BP	130	4	0.0041976
GO:0035296	regulation of tube diameter	BP	130	4	0.0041976
GO:0032940	secretion by cell	BP	1398	15	0.0042342
GO:0003013	circulatory system process	BP	511	8	0.0042509
GO:0018130	heterocycle biosynthetic process	BP	4211	33	0.0043619
GO:0048666	neuron development	BP	999	12	0.004373

GO:2000026	regulation of multicellular organisma…	BP	1835	18	0.0044687
GO:0019438	aromatic compound biosynthetic proces…	BP	4218	33	0.0044788
GO:0007423	sensory organ development	BP	516	8	0.0045044
GO:0065007	biological regulation	BP	11517	72	0.0045775
GO:0031175	neuron projection development	BP	878	11	0.0046386
GO:0030574	collagen catabolic process	BP	67	3	0.0046616
GO:0097061	dendritic spine organization	BP	67	3	0.0046616
GO:0009583	detection of light stimulus	BP	67	3	0.0046616
GO:0042060	wound healing	BP	519	8	0.004662
GO:0040008	regulation of growth	BP	635	9	0.0047132
GO:0006865	amino acid transport	BP	135	4	0.0047978
GO:0007612	learning	BP	136	4	0.0049244
GO:0060078	regulation of postsynaptic membrane p…	BP	136	4	0.0049244
GO:0046425	regulation of JAK-STAT cascade	BP	137	4	0.0050532
GO:1904892	regulation of STAT cascade	BP	137	4	0.0050532
GO:0046483	heterocycle metabolic process	BP	5819	42	0.0050885
GO:0031399	regulation of protein modification pr…	BP	1713	17	0.0051207
GO:0050880	regulation of blood vessel size	BP	138	4	0.0051842
GO:0106027	neuron projection organization	BP	70	3	0.0052693
GO:0010975	regulation of neuron projection devel…	BP	420	7	0.0052978
GO:0035150	regulation of tube size	BP	139	4	0.0053175
GO:0051239	regulation of multicellular organisma…	BP	2786	24	0.0053256
GO:0006139	nucleobase-containing compound metabo…	BP	5657	41	0.005362
GO:0045981	positive regulation of nucleotide met…	BP	140	4	0.0054531
GO:1900544	positive regulation of purine nucleot…	BP	140	4	0.0054531
GO:0009628	response to abiotic stimulus	BP	1162	13	0.0054892
GO:0048513	animal organ development	BP	3281	27	0.005637
GO:0030155	regulation of cell adhesion	BP	655	9	0.0057469
GO:0007596	blood coagulation	BP	323	6	0.0058139
GO:0034109	homotypic cell-cell adhesion	BP	73	3	0.0059224
GO:0007409	axonogenesis	BP	431	7	0.0060795
GO:0050817	coagulation	BP	327	6	0.0061637
GO:0014070	response to organic cyclic compound	BP	914	11	0.0062281

GO:0007166	cell surface receptor signaling pathw…	BP	2663	23	0.0062329
GO:0044236	multicellular organism metabolic proc…	BP	146	4	0.0063155
GO:0044243	multicellular organismal catabolic pr…	BP	75	3	0.0063836
GO:0051952	regulation of amine transport	BP	75	3	0.0063836
GO:0044283	small molecule biosynthetic process	BP	549	8	0.0064822
GO:0043270	positive regulation of ion transport	BP	234	5	0.0065591
GO:2001022	positive regulation of response to DN…	BP	77	3	0.0068656
GO:0022408	negative regulation of cell-cell adhe…	BP	150	4	0.0069381
GO:0002695	negative regulation of leukocyte acti…	BP	150	4	0.0069381
GO:0007162	negative regulation of cell adhesion	BP	238	5	0.0070332
GO:0001932	regulation of protein phosphorylation	BP	1337	14	0.0070372
GO:0043009	chordate embryonic development	BP	557	8	0.0070483
GO:0006351	transcription, DNA-templated	BP	3667	29	0.0070507
GO:0031345	negative regulation of cell projectio…	BP	151	4	0.0070998
GO:0006355	regulation of transcription, DNA-temp…	BP	3508	28	0.0072439
GO:0008285	negative regulation of cell prolifera…	BP	680	9	0.0072771
GO:0051091	positive regulation of DNA binding tr…	BP	240	5	0.0072791
GO:1903076	regulation of protein localization to…	BP	79	3	0.0073686
GO:0009792	embryo development ending in birth or…	BP	562	8	0.0074206
GO:0097659	nucleic acid-templated transcription	BP	3683	29	0.007491
GO:0009987	cellular process	BP	15094	88	0.0075323
GO:0120035	regulation of plasma membrane bounded…	BP	564	8	0.0075736
GO:0042221	response to chemical	BP	4192	32	0.0075751
GO:0030307	positive regulation of cell growth	BP	154	4	0.0076
GO:0097435	supramolecular fiber organization	BP	565	8	0.007651
GO:0030168	platelet activation	BP	155	4	0.0077718
GO:1903506	regulation of nucleic acid-templated …	BP	3529	28	0.0078531
GO:0050810	regulation of steroid biosynthetic pr…	BP	81	3	0.007893
GO:0048518	positive regulation of biological pro…	BP	5423	39	0.0079165
GO:0032774	RNA biosynthetic process	BP	3699	29	0.0079543
GO:0045664	regulation of neuron differentiation	BP	569	8	0.0079666
GO:0006357	regulation of transcription from RNA …	BP	1944	18	0.0080347
GO:2001141	regulation of RNA biosynthetic proces…	BP	3537	28	0.0080961

GO:0007519	skeletal muscle tissue development	BP	157	4	0.0081229
GO:0120036	plasma membrane bounded cell projecti…	BP	1363	14	0.0082756
GO:2001242	regulation of intrinsic apoptotic sig…	BP	158	4	0.0083023
GO:2000027	regulation of organ morphogenesis	BP	248	5	0.0083226
GO:1902533	positive regulation of intracellular …	BP	952	11	0.0083435
GO:0015837	amine transport	BP	83	3	0.0084389
GO:0050886	endocrine process	BP	83	3	0.0084389
GO:0031344	regulation of cell projection organiz…	BP	575	8	0.0084583
GO:0007259	JAK-STAT cascade	BP	159	4	0.0084843
GO:0097696	STAT cascade	BP	159	4	0.0084843
GO:0006469	negative regulation of protein kinase…	BP	250	5	0.0085989
GO:0003018	vascular process in circulatory syste…	BP	160	4	0.0086689
GO:0051252	regulation of RNA metabolic process	BP	3723	29	0.0086939
GO:0032844	regulation of homeostatic process	BP	464	7	0.0089452
GO:0030193	regulation of blood coagulation	BP	85	3	0.0090065
GO:0019217	regulation of fatty acid metabolic pr…	BP	85	3	0.0090065
GO:1900046	regulation of hemostasis	BP	85	3	0.0090065
GO:0097006	regulation of plasma lipoprotein part…	BP	86	3	0.0092985
GO:0061564	axon development	BP	468	7	0.0093502
GO:0006835	dicarboxylic acid transport	BP	87	3	0.0095959
GO:1904375	regulation of protein localization to…	BP	87	3	0.0095959
GO:0051128	regulation of cellular component orga…	BP	2288	20	0.0096156
GO:0006366	transcription from RNA polymerase II …	BP	2133	19	0.0096167
GO:0060538	skeletal muscle organ development	BP	165	4	0.0096312
GO:0008283	cell proliferation	BP	1982	18	0.009722
GO:0030030	cell projection organization	BP	1392	14	0.0098558
GO:0006112	energy reserve metabolic process	BP	88	3	0.0098989
GO:0003073	regulation of systemic arterial blood…	BP	88	3	0.0098989

Table S2D. Enriched biological pathways based on *hyper*methylated DMRs in subcutaneous adipose tissue after sleep loss compared with sleep.

GO term ID	Term name	Namespace	N	DE	q value
GO:0050877	nervous system process	BP	1217	15	0.0000157
GO:0050804	modulation of chemical synaptic trans…	BP	306	7	0.0000922
GO:0003008	system process	BP	1953	18	0.0000962
GO:0050806	positive regulation of synaptic trans…	BP	134	5	0.000103
GO:0007605	sensory perception of sound	BP	143	5	0.0001398
GO:1901700	response to oxygen-containing compoun…	BP	1512	15	0.0001853
GO:0009605	response to external stimulus	BP	2071	18	0.000202
GO:0050954	sensory perception of mechanical stim…	BP	160	5	0.0002359
GO:0033993	response to lipid	BP	893	11	0.0002451
GO:0033273	response to vitamin	BP	90	4	0.0002711
GO:0023051	regulation of signaling	BP	3363	24	0.0002951
GO:0010648	negative regulation of cell communica…	BP	1274	13	0.0004039
GO:0023057	negative regulation of signaling	BP	1278	13	0.0004161
GO:0000904	cell morphogenesis involved in differ…	BP	658	9	0.0004432
GO:0030199	collagen fibril organization	BP	43	3	0.0004459
GO:0010646	regulation of cell communication	BP	3314	23	0.0006188
GO:0009628	response to abiotic stimulus	BP	1162	12	0.0006215
GO:0022610	biological adhesion	BP	1339	13	0.0006463
GO:0046426	negative regulation of JAK-STAT casca…	BP	50	3	0.000696
GO:1904893	negative regulation of STAT cascade	BP	50	3	0.000696
GO:0007409	axonogenesis	BP	431	7	0.0007336
GO:0050953	sensory perception of light stimulus	BP	206	5	0.0007482
GO:0009581	detection of external stimulus	BP	124	4	0.0009106
GO:0034381	plasma lipoprotein particle clearance	BP	55	3	0.0009201
GO:0006820	anion transport	BP	587	8	0.0009573
GO:0009582	detection of abiotic stimulus	BP	127	4	0.0009954
GO:0061564	axon development	BP	468	7	0.0011841
GO:0007612	learning	BP	136	4	0.0012827
GO:0007611	learning or memory	BP	233	5	0.0012958
GO:0015909	long-chain fatty acid transport	BP	62	3	0.0013036

GO:0046425	regulation of JAK-STAT cascade	BP	137	4	0.0013178
GO:1904892	regulation of STAT cascade	BP	137	4	0.0013178
GO:0061448	connective tissue development	BP	235	5	0.0013457
GO:0048585	negative regulation of response to st…	BP	1458	13	0.0014125
GO:0035556	intracellular signal transduction	BP	2659	19	0.0014992
GO:0023052	signaling	BP	6178	34	0.0015402
GO:0009583	detection of light stimulus	BP	67	3	0.0016308
GO:0009653	anatomical structure morphogenesis	BP	2470	18	0.0016455
GO:1902532	negative regulation of intracellular …	BP	503	7	0.0017876
GO:0015718	monocarboxylic acid transport	BP	153	4	0.0019755
GO:0007155	cell adhesion	BP	1332	12	0.00201
GO:0022603	regulation of anatomical structure mo…	BP	982	10	0.0020245
GO:0007519	skeletal muscle tissue development	BP	157	4	0.0021699
GO:0010033	response to organic substance	BP	2965	20	0.0022079
GO:0009968	negative regulation of signal transdu…	BP	1169	11	0.0022356
GO:0007259	JAK-STAT cascade	BP	159	4	0.0022718
GO:0097696	STAT cascade	BP	159	4	0.0022718
GO:0048667	cell morphogenesis involved in neuron…	BP	527	7	0.0023237
GO:0022414	reproductive process	BP	1356	12	0.0023317
GO:0000003	reproduction	BP	1357	12	0.002346
GO:1901701	cellular response to oxygen-containin…	BP	1005	10	0.0023964
GO:0050890	cognition	BP	270	5	0.0024672
GO:0008150	biological_process	BP	16519	68	0.0024837
GO:0032102	negative regulation of response to ex…	BP	272	5	0.002547
GO:0007267	cell-cell signaling	BP	1561	13	0.0025868
GO:0060538	skeletal muscle organ development	BP	165	4	0.0025975
GO:0032989	cellular component morphogenesis	BP	1018	10	0.0026299
GO:1902531	regulation of intracellular signal tr…	BP	1772	14	0.0028381
GO:0009966	regulation of signal transduction	BP	3031	20	0.0028691
GO:0007584	response to nutrient	BP	170	4	0.0028923
GO:0007600	sensory perception	BP	873	9	0.0031521
GO:0071396	cellular response to lipid	BP	558	7	0.0031914
GO:0030193	regulation of blood coagulation	BP	85	3	0.0032159

GO:1900046	regulation of hemostasis	BP	85	3	0.0032159
GO:0097006	regulation of plasma lipoprotein part…	BP	86	3	0.0033239
GO:0007154	cell communication	BP	6196	33	0.0033866
GO:0097435	supramolecular fiber organization	BP	565	7	0.0034178
GO:0050896	response to stimulus	BP	8322	41	0.0034528
GO:0051216	cartilage development	BP	180	4	0.0035492
GO:0009416	response to light stimulus	BP	294	5	0.0035533
GO:0007610	behavior	BP	572	7	0.0036563
GO:0050818	regulation of coagulation	BP	89	3	0.0036612
GO:0021549	cerebellum development	BP	90	3	0.0037781
GO:0015908	fatty acid transport	BP	90	3	0.0037781
GO:0009314	response to radiation	BP	432	6	0.0038571
GO:0007565	female pregnancy	BP	186	4	0.0039885
GO:0046942	carboxylic acid transport	BP	303	5	0.0040377
GO:1905114	cell surface receptor signaling pathw…	BP	585	7	0.0041328
GO:0098869	cellular oxidant detoxification	BP	93	3	0.0041424
GO:0002062	chondrocyte differentiation	BP	93	3	0.0041424
GO:0048812	neuron projection morphogenesis	BP	587	7	0.0042101
GO:0000902	cell morphogenesis	BP	921	9	0.0044768
GO:0015849	organic acid transport	BP	311	5	0.0045064
GO:0050905	neuromuscular process	BP	96	3	0.0045274
GO:0001763	morphogenesis of a branching structur…	BP	193	4	0.0045459
GO:0015711	organic anion transport	BP	449	6	0.0046494
GO:1990748	cellular detoxification	BP	97	3	0.0046604
GO:0098916	anterograde trans-synaptic signaling	BP	600	7	0.0047397
GO:0007268	chemical synaptic transmission	BP	600	7	0.0047397
GO:0120039	plasma membrane bounded cell projecti…	BP	601	7	0.0047824
GO:0022037	metencephalon development	BP	98	3	0.0047957
GO:0099536	synaptic signaling	BP	602	7	0.0048255
GO:0099537	trans-synaptic signaling	BP	602	7	0.0048255
GO:0048858	cell projection morphogenesis	BP	604	7	0.0049124
GO:0098754	detoxification	BP	101	3	0.0052158
GO:0007601	visual perception	BP	202	4	0.0053367

GO:0009612	response to mechanical stimulus	BP	205	4	0.0056196
GO:0030154	cell differentiation	BP	3908	23	0.0056336
GO:0030198	extracellular matrix organization	BP	329	5	0.0057011
GO:0043062	extracellular structure organization	BP	330	5	0.0057735
GO:0032990	cell part morphogenesis	BP	623	7	0.0057985
GO:0097237	cellular response to toxic substance	BP	105	3	0.0058095
GO:0044070	regulation of anion transport	BP	105	3	0.0058095
GO:0032502	developmental process	BP	5921	31	0.006414
GO:0048468	cell development	BP	1944	14	0.0064677
GO:0042221	response to chemical	BP	4192	24	0.0065089
GO:0044706	multi-multicellular organism process	BP	215	4	0.0066344
GO:0001501	skeletal system development	BP	486	6	0.0067816
GO:0009887	animal organ morphogenesis	BP	985	9	0.0068808
GO:0099565	chemical synaptic transmission, posts…	BP	114	3	0.0072888
GO:0065007	biological regulation	BP	11517	51	0.0075926
GO:0048699	generation of neurons	BP	1378	11	0.0076871
GO:0003231	cardiac ventricle development	BP	119	3	0.0081983
GO:0007399	nervous system development	BP	2211	15	0.0082159
GO:0014706	striated muscle tissue development	BP	360	5	0.0082573
GO:0032963	collagen metabolic process	BP	120	3	0.0083878
GO:0048856	anatomical structure development	BP	5518	29	0.0084578
GO:0032501	multicellular organismal process	BP	7084	35	0.0086641
GO:0050680	negative regulation of epithelial cel…	BP	122	3	0.0087747
GO:0070887	cellular response to chemical stimulu…	BP	2892	18	0.0088916
GO:0007423	sensory organ development	BP	516	6	0.0089735
GO:0044259	multicellular organismal macromolecul…	BP	125	3	0.0093743
GO:0098657	import into cell	BP	683	7	0.0093939
GO:0007275	multicellular organism development	BP	5056	27	0.0094175
GO:0048869	cellular developmental process	BP	4078	23	0.0094735
GO:0010647	positive regulation of cell communica…	BP	1619	12	0.0094854
GO:0023056	positive regulation of signaling	BP	1625	12	0.009753
GO:0051094	positive regulation of developmental …	BP	1233	10	0.0099083

Table S2E. Enriched biological pathways based on *hypo*methylated DMRs in subcutaneous adipose tissue after sleep loss compared with sleep.

GO term	Term	Namespace	N	DE	q value
GO:0043517	positive regulation of DNA damage res…	BP	14	3	0.0000013
GO:1901798	positive regulation of signal transdu…	BP	21	3	0.0000049
GO:0051216	cartilage development	BP	180	5	0.0000095
GO:0043516	regulation of DNA damage response, si…	BP	30	3	0.0000148
GO:0048705	skeletal system morphogenesis	BP	210	5	0.00002
GO:2001233	regulation of apoptotic signaling pat…	BP	378	6	0.0000273
GO:0097190	apoptotic signaling pathway	BP	584	7	0.0000329
GO:0061448	connective tissue development	BP	235	5	0.0000343
GO:0001501	skeletal system development	BP	486	6	0.0001099
GO:0045861	negative regulation of proteolysis	BP	335	5	0.0001822
GO:0060348	bone development	BP	183	4	0.0002025
GO:0019216	regulation of lipid metabolic process	BP	358	5	0.0002477
GO:2001022	positive regulation of response to DN…	BP	77	3	0.0002527
GO:0019217	regulation of fatty acid metabolic pr…	BP	85	3	0.0003382
GO:0060349	bone morphogenesis	BP	88	3	0.0003746
GO:0007631	feeding behavior	BP	108	3	0.0006817
GO:0030330	DNA damage response, signal transduct…	BP	109	3	0.0007003
GO:0045595	regulation of cell differentiation	BP	1649	9	0.0009084
GO:0050878	regulation of body fluid levels	BP	480	5	0.0009398
GO:0045834	positive regulation of lipid metaboli…	BP	123	3	0.0009941
GO:0042770	signal transduction in response to DN…	BP	123	3	0.0009941
GO:0097193	intrinsic apoptotic signaling pathway	BP	290	4	0.0011452
GO:0097746	regulation of blood vessel diameter	BP	130	3	0.0011662
GO:0035296	regulation of tube diameter	BP	130	3	0.0011662
GO:0010646	regulation of cell communication	BP	3314	13	0.0012232
GO:0050880	regulation of blood vessel size	BP	138	3	0.0013848

GO:0023051	regulation of signaling	BP	3363	13	0.0014051
GO:0035150	regulation of tube size	BP	139	3	0.0014138
GO:0045981	positive regulation of nucleotide met…	BP	140	3	0.0014432
GO:1900544	positive regulation of purine nucleot…	BP	140	3	0.0014432
GO:0002695	negative regulation of leukocyte acti…	BP	150	3	0.0017583
GO:0007599	hemostasis	BP	328	4	0.0017994
GO:0030154	cell differentiation	BP	3908	14	0.0018045
GO:0007188	adenylate cyclase-modulating G-protei…	BP	153	3	0.0018605
GO:0034641	cellular nitrogen compound metabolic …	BP	6434	19	0.001894
GO:0030307	positive regulation of cell growth	BP	154	3	0.0018954
GO:0006915	apoptotic process	BP	1840	9	0.0019667
GO:0009967	positive regulation of signal transdu…	BP	1483	8	0.0019915
GO:0007610	behavior	BP	572	5	0.0020387
GO:2001242	regulation of intrinsic apoptotic sig…	BP	158	3	0.0020391
GO:0003018	vascular process in circulatory syste…	BP	160	3	0.0021134
GO:0010565	regulation of cellular ketone metabol…	BP	165	3	0.0023065
GO:0046890	regulation of lipid biosynthetic proc…	BP	166	3	0.0023463
GO:0050866	negative regulation of cell activatio…	BP	169	3	0.0024686
GO:0090304	nucleic acid metabolic process	BP	5008	16	0.0024882
GO:0048856	anatomical structure development	BP	5518	17	0.0025028
GO:2001235	positive regulation of apoptotic sign…	BP	174	3	0.0026809
GO:0051129	negative regulation of cellular compo…	BP	611	5	0.002714
GO:2001020	regulation of response to DNA damage …	BP	175	3	0.0027247
GO:1901796	regulation of signal transduction by …	BP	175	3	0.0027247
GO:0048869	cellular developmental process	BP	4078	14	0.0027367
GO:0051783	regulation of nuclear division	BP	179	3	0.0029043
GO:0007187	G-protein coupled receptor signaling …	BP	180	3	0.0029503
GO:0001558	regulation of cell growth	BP	380	4	0.0030641
GO:0012501	programmed cell death	BP	1969	9	0.0031295

GO:0002683	negative regulation of immune system …	BP	387	4	0.0032712
GO:0006139	nucleobase-containing compound metabo…	BP	5657	17	0.0033214
GO:0040007	growth	BP	937	6	0.0034061
GO:0010647	positive regulation of cell communica…	BP	1619	8	0.0034437
GO:0023056	positive regulation of signaling	BP	1625	8	0.003523
GO:0007626	locomotory behavior	BP	192	3	0.0035377
GO:1903530	regulation of secretion by cell	BP	653	5	0.0036098
GO:0001775	cell activation	BP	1279	7	0.0036583
GO:0023061	signal release	BP	417	4	0.0042673
GO:0009653	anatomical structure morphogenesis	BP	2470	10	0.0042875
GO:0009887	animal organ morphogenesis	BP	985	6	0.0043522
GO:0048732	gland development	BP	421	4	0.0044141
GO:2001234	negative regulation of apoptotic sign…	BP	209	3	0.004485
GO:0046483	heterocycle metabolic process	BP	5819	17	0.0045548
GO:0007155	cell adhesion	BP	1332	7	0.0045755
GO:0022610	biological adhesion	BP	1339	7	0.0047087
GO:0008219	cell death	BP	2094	9	0.0047278
GO:0006725	cellular aromatic compound metabolic …	BP	5857	17	0.0048946
GO:0051716	cellular response to stimulus	BP	6947	19	0.0049542
GO:0080134	regulation of response to stress	BP	1353	7	0.004984
GO:0048522	positive regulation of cellular proce…	BP	4846	15	0.0050759
GO:0051046	regulation of secretion	BP	711	5	0.0051746
GO:0032502	developmental process	BP	5921	17	0.0055155
GO:0042180	cellular ketone metabolic process	BP	229	3	0.0057798
GO:0032940	secretion by cell	BP	1398	7	0.0059523
GO:0009966	regulation of signal transduction	BP	3031	11	0.0060938
GO:0016049	cell growth	BP	474	4	0.0066913
GO:0030162	regulation of proteolysis	BP	758	5	0.0067581
GO:0010817	regulation of hormone levels	BP	481	4	0.0070409

GO:0045927	positive regulation of growth	BP	248	3	0.0071981
GO:1901360	organic cyclic compound metabolic pro…	BP	6069	17	0.0072099
GO:0050896	response to stimulus	BP	8322	21	0.0072777
GO:0042981	regulation of apoptotic process	BP	1459	7	0.0074849
GO:0046883	regulation of hormone secretion	BP	252	3	0.0075207
GO:0007275	multicellular organism development	BP	5056	15	0.0076765
GO:0006974	cellular response to DNA damage stimu…	BP	782	5	0.0076864
GO:1900542	regulation of purine nucleotide metab…	BP	255	3	0.0077682
GO:0006996	organelle organization	BP	3595	12	0.0078426
GO:0022008	neurogenesis	BP	1472	7	0.0078466
GO:0043067	regulation of programmed cell death	BP	1474	7	0.0079033
GO:0006950	response to stress	BP	3616	12	0.0082168
GO:0006140	regulation of nucleotide metabolic pr…	BP	262	3	0.0083644
GO:0008015	blood circulation	BP	506	4	0.0083881
GO:0045321	leukocyte activation	BP	1131	6	0.0084427
GO:0044092	negative regulation of molecular func…	BP	1135	6	0.0085841
GO:0003013	circulatory system process	BP	511	4	0.0086765
GO:0072331	signal transduction by p53 class medi…	BP	268	3	0.0088964
GO:0090068	positive regulation of cell cycle pro…	BP	269	3	0.0089869
GO:0009888	tissue development	BP	1901	8	0.0090181
GO:0050890	cognition	BP	270	3	0.009078
GO:0060284	regulation of cell development	BP	815	5	0.0091044
GO:0042060	wound healing	BP	519	4	0.0091514
GO:0046903	secretion	BP	1528	7	0.0095562
GO:0043066	negative regulation of apoptotic proc…	BP	828	5	0.00971

Table S2F. CpG probes closest to reaching significance in skeletal muscle in response to sleep loss compared with sleep.

Probe	Chr	position	logFC	Average expression	t	P-value	q value
cg02934600	chr1	107600376	0.02753258	0.34215503	6.774544	3.94E-06	0.9988396
cg06070414	chr7	95226412	0.04423437	0.24776351	6.493057	6.61E-06	0.9988396
cg00722081	chr10	61147668	-0.02842205	0.62892642	-6.327758	9.00E-06	0.9988396
cg26493306	chr5	134463458	0.02261804	0.9203585	6.275672	9.92E-06	0.9988396
cg04957146	chr17	2551652	0.02149195	0.87135571	6.164014	1.23E-05	0.9988396
cg01051642	chr1	2517410	0.02560049	0.11585213	6.000548	1.67E-05	0.9988396
cg09250087	chr2	161127564	0.02914209	0.69137042	5.862363	2.19E-05	0.9988396
cg20292318	chr17	77141853	-0.02535266	0.81763694	-5.494034	4.51E-05	0.9988396
cg10747185	chr3	176862267	0.03792301	0.83633599	5.493864	4.51E-05	0.9988396
cg03063453	chr19	52693134	0.02288002	0.13384391	5.490893	4.53E-05	0.9988396
cg23335976	chr10	18240598	0.03056735	0.80908058	5.471804	4.71E-05	0.9988396
cg26497185	chr10	125819893	0.0345724	0.79512816	5.385925	5.59E-05	0.9988396
cg20983329	chrX	70338670	0.04096218	0.3271348	5.345167	6.07E-05	0.9988396
cg17804627	chr1	35325459	-0.01576963	0.05522482	-5.306514	6.56E-05	0.9988396
cg25013978	chr5	36149258	0.02967198	0.71095467	5.286903	6.82E-05	0.9988396
cg16328558	chr1	45766469	0.02206586	0.85455378	5.283494	6.87E-05	0.9988396
cg26794871	chr20	44934712	-0.03087938	0.70890816	-5.245018	7.42E-05	0.9988396
cg11759293	chr13	73359517	0.02022863	0.85704316	5.184951	8.38E-05	0.9988396
cg05516004	chr21	46496180	-0.0348843	0.72435047	-5.183919	8.40E-05	0.9988396
cg06135689	chr17	35085060	-0.03399909	0.26722348	-5.177792	8.50E-05	0.9988396

Table S3. Differentially expressed genes in skeletal muscle and subcutaneous adipose tissue in response to acute sleep loss. Showing genes that are either (**A**) upregulated or (**B**) downregulated in skeletal muscle; as well as (**C**) upregulated or (**D**) downregulated genes in subcutaneous adipose tissue, based on RNA-seq of samples obtained after sleep loss compared with after normal sleep, and for transcripts with adjusted (FDR) P-values<0.05. For each gene, the following information is also listed: log fold change (fc); log counts per million (cpm); likelihood ratio (LR) statistics value; the raw and adjusted (FDR) P-values; and the Ensembl and Entrez gene ids.

Table S3A. Upregulated gene transcripts in skeletal muscle after sleep loss compared with normal sleep.

Gene name	log fc	log cpm	LR	P-value	FDR	Ensembl gene id	Entrez id
PDK4	1.71	8.83	34.54	4.18E-09	5.25E-05	ENSG00000004799	5166
FZD4	0.39	6.42	19.93	8.02E-06	7.19E-03	ENSG00000174804	8322
MGAM	1.43	-0.14	17.59	2.75E-05	1.32E-02	ENSG00000257335	8972
CISH	1.34	2.77	15.40	8.72E-05	2.28E-02	ENSG00000114737	1154
CXCR2	1.11	0.09	15.40	8.72E-05	2.28E-02	ENSG00000180871	3579
TXNIP	0.50	10.26	14.30	1.56E-04	3.27E-02	ENSG00000117289	10628
KANK1	0.25	5.58	14.27	1.59E-04	3.27E-02	ENSG00000107104	23189
TMEM154	0.77	0.60	14.21	1.63E-04	3.31E-02	ENSG00000170006	201799
PFKFB3	0.98	6.04	13.78	2.06E-04	3.64E-02	ENSG00000170525	5209
NNMT	0.97	2.27	13.72	2.12E-04	3.69E-02	ENSG00000166741	4837
USP6NL	0.50	1.78	13.58	2.29E-04	3.83E-02	ENSG00000148429	9712
CPT1A	0.43	3.59	13.15	2.87E-04	4.19E-02	ENSG00000110090	1374
FZD5	0.54	2.33	13.07	3.00E-04	4.19E-02	ENSG00000163251	7855
PPP2R1B	0.41	4.09	12.91	3.27E-04	4.23E-02	ENSG00000137713	5519
CYSLTR1	0.96	0.14	12.65	3.75E-04	4.50E-02	ENSG00000173198	10800
MAP9	0.68	0.33	12.49	4.08E-04	4.70E-02	ENSG00000164114	79884
MTURN	0.35	5.76	12.44	4.20E-04	4.70E-02	ENSG00000180354	222166
MED12L	1.48	0.21	12.36	4.39E-04	4.70E-02	ENSG00000144893	116931

LRRK2	0.24	5.06	12.35	4.41E-04	4.70E-02	ENSG00000188906	120892
FCGR3B	0.99	0.57	12.35	4.41E-04	4.70E-02	ENSG00000162747	2215

Table S3B. Downregulated gene transcripts in skeletal muscle after sleep loss compared with normal sleep.

Gene name	log fc	log cpm	LR	P-value	FDR	Ensembl gene id	Entrez id
FAM78A	-0.52	5.14	26.71	2.37E-07	1.49E-03	ENSG00000126882	286336
TFRC	-0.64	6.94	25.19	5.18E-07	1.94E-03	ENSG00000072274	7037
PPP1R3C	-0.73	9.36	24.86	6.17E-07	1.94E-03	ENSG00000119938	5507
JUND	-0.40	3.46	22.25	2.40E-06	5.36E-03	ENSG00000130522	3727
MIDN	-0.71	3.29	22.12	2.56E-06	5.36E-03	ENSG00000167470	90007
PKDCC	-0.39	5.36	21.16	4.23E-06	5.60E-03	ENSG00000162878	91461
TESK1	-0.39	3.92	20.94	4.74E-06	5.60E-03	ENSG00000107140	7016
NPHP1	-0.43	6.13	20.90	4.83E-06	5.60E-03	ENSG00000144061	4867
PTP4A3	-0.48	7.14	20.72	5.32E-06	5.60E-03	ENSG00000184489	11156
PROB1	-0.65	3.98	20.60	5.65E-06	5.60E-03	ENSG00000228672	389333
SMTNL2	-0.49	6.89	20.60	5.65E-06	5.60E-03	ENSG00000188176	342527
TNK2	-0.43	4.63	20.55	5.80E-06	5.60E-03	ENSG00000061938	10188
PLEKHH3	-0.53	3.77	19.74	8.86E-06	7.42E-03	ENSG00000068137	79990
SH3RF3	-0.55	2.85	19.56	9.76E-06	7.66E-03	ENSG00000172985	344558
KCNJ11	-0.49	5.23	19.14	1.21E-05	8.97E-03	ENSG00000187486	3767
HES1	-0.52	2.93	18.78	1.47E-05	1.02E-02	ENSG00000114315	3280
BCAR1	-0.48	4.27	18.54	1.66E-05	1.07E-02	ENSG00000050820	9564
ZBTB7B	-0.42	3.51	18.41	1.78E-05	1.07E-02	ENSG00000160685	51043
SMTN	-0.40	5.30	18.40	1.79E-05	1.07E-02	ENSG00000183963	6525
RGMA	-0.45	4.74	18.25	1.94E-05	1.10E-02	ENSG00000182175	56963
SLC45A3	-0.69	1.68	18.18	2.01E-05	1.10E-02	ENSG00000158715	85414
ZNF865	-0.54	1.66	18.09	2.10E-05	1.10E-02	ENSG00000261221	100507290

DOK7	-0.60	2.84	17.98	2.23E-05	1.12E-02	ENSG00000175920	285489
C20orf166	-0.40	6.43	17.48	2.91E-05	1.32E-02	ENSG00000174407	128826
FHL3	-0.44	8.17	17.45	2.94E-05	1.32E-02	ENSG00000183386	2275
PPP1R16A	-0.56	3.63	17.28	3.23E-05	1.40E-02	ENSG00000160972	84988
SPEG	-0.51	7.67	17.22	3.33E-05	1.40E-02	ENSG00000072195	10290
SNAI3	-0.87	2.54	16.99	3.77E-05	1.52E-02	ENSG00000185669	333929
MAP1S	-0.55	1.92	16.90	3.95E-05	1.52E-02	ENSG00000130479	55201
OSBPL7	-0.40	4.04	16.88	3.99E-05	1.52E-02	ENSG00000006025	114881
MTSS1L	-0.48	4.66	16.78	4.19E-05	1.54E-02	ENSG00000132613	92154
MIIP	-0.43	2.76	16.73	4.31E-05	1.54E-02	ENSG00000116691	60672
NEURL1	-0.40	5.58	16.65	4.48E-05	1.56E-02	ENSG00000107954	9148
GNA11	-0.40	4.96	16.33	5.33E-05	1.77E-02	ENSG00000088256	2767
WNK2	-0.44	4.43	16.27	5.49E-05	1.77E-02	ENSG00000165238	65268
MYADML2	-0.54	4.88	16.24	5.57E-05	1.77E-02	ENSG00000185105	255275
TEAD3	-0.39	3.19	16.22	5.63E-05	1.77E-02	ENSG00000007866	7005
C15orf27	-0.48	3.33	16.06	6.13E-05	1.88E-02	ENSG00000169758	123591
FAM53B	-0.38	4.98	15.79	7.08E-05	2.11E-02	ENSG00000189319	9679
RNF126	-0.48	3.02	15.69	7.45E-05	2.11E-02	ENSG00000070423	55658
HEXIM2	-0.47	3.43	15.69	7.47E-05	2.11E-02	ENSG00000168517	124790
AHDC1	-0.42	3.88	15.67	7.55E-05	2.11E-02	ENSG00000126705	27245
RFNG	-0.41	3.17	15.52	8.18E-05	2.23E-02	ENSG00000169733	5986
HMGA1	-0.38	3.80	15.34	8.98E-05	2.29E-02	ENSG00000137309	3159
TFEB	-0.40	4.76	15.31	9.13E-05	2.29E-02	ENSG00000112561	7942
JSRP1	-0.68	4.93	14.98	1.09E-04	2.68E-02	ENSG00000167476	126306
MLF1	-0.47	6.07	14.85	1.17E-04	2.82E-02	ENSG00000178053	4291
ADAMTSL5	-0.53	1.90	14.76	1.22E-04	2.84E-02	ENSG00000185761	339366
ATAD3A	-0.43	2.55	14.76	1.22E-04	2.84E-02	ENSG00000197785	55210
HSPA1A	-0.35	4.61	14.43	1.45E-04	3.27E-02	ENSG00000204389	3303

MPST	-0.37	3.92	14.38	1.49E-04	3.27E-02	ENSG00000128309	4357
KLHL25	-0.56	2.10	14.38	1.49E-04	3.27E-02	ENSG00000183655	64410
CITED4	-0.57	2.35	14.33	1.53E-04	3.27E-02	ENSG00000179862	163732
MPP7	-0.28	4.96	14.27	1.59E-04	3.27E-02	ENSG00000150054	143098
STEAP3	-0.34	4.55	14.18	1.67E-04	3.32E-02	ENSG00000115107	55240
PCBP4	-0.34	5.14	14.13	1.71E-04	3.35E-02	ENSG00000090097	57060
ST3GAL2	-0.35	4.57	14.08	1.75E-04	3.39E-02	ENSG00000157350	6483
CCDC85B	-0.62	1.44	13.90	1.93E-04	3.64E-02	ENSG00000175602	11007
GLTPD1	-0.49	3.87	13.88	1.95E-04	3.64E-02	ENSG00000224051	80772
RASL12	-0.38	3.90	13.85	1.98E-04	3.64E-02	ENSG00000103710	51285
BTBD2	-0.40	4.17	13.80	2.03E-04	3.64E-02	ENSG00000133243	55643
ZNF787	-0.48	3.18	13.79	2.05E-04	3.64E-02	ENSG00000142409	126208
ZNF784	-0.39	3.18	13.70	2.15E-04	3.69E-02	ENSG00000179922	147808
TBX1	-0.55	2.56	13.58	2.28E-04	3.83E-02	ENSG00000184058	6899
C1orf170	-0.47	6.64	13.53	2.35E-04	3.86E-02	ENSG00000187642	84808
PPP1R3F	-0.37	3.50	13.51	2.37E-04	3.86E-02	ENSG00000049769	89801
ABTB2	-0.41	2.64	13.47	2.43E-04	3.91E-02	ENSG00000166016	25841
FAM47E-STBD1	-0.40	3.83	13.44	2.46E-04	3.91E-02	ENSG00000118804	8987
LRP3	-0.46	3.33	13.38	2.55E-04	4.00E-02	ENSG00000130881	4037
MIB2	-0.52	4.90	13.32	2.63E-04	4.08E-02	ENSG00000197530	142678
PPAPDC3	-0.41	6.34	13.20	2.79E-04	4.19E-02	ENSG00000160539	84814
SCRIB	-0.49	3.96	13.17	2.84E-04	4.19E-02	ENSG00000180900	23513
ARX	-0.53	2.02	13.14	2.89E-04	4.19E-02	ENSG00000004848	170302
CCDC85C	-0.43	2.97	13.06	3.02E-04	4.19E-02	ENSG00000205476	317762
ACSL6	-0.42	1.98	13.03	3.07E-04	4.19E-02	ENSG00000164398	23305
FAM195A	-0.44	4.44	13.03	3.07E-04	4.19E-02	ENSG00000172366	84331
TUBB4B	-0.40	5.24	13.02	3.07E-04	4.19E-02	ENSG00000188229	10383
PIK3C2B	-0.29	5.52	13.02	3.08E-04	4.19E-02	ENSG00000133056	5287

ORAI1	-0.44	3.97	13.01	3.10E-04	4.19E-02	ENSG00000182500		84876
SBK1	-0.48	3.67	13.01	3.10E-04	4.19E-02	ENSG00000188322		388228
ZNF524	-0.44	2.61	12.97	3.16E-04	4.20E-02	ENSG00000171443		147807
P2RY2	-0.39	3.87	12.96	3.18E-04	4.20E-02	ENSG00000175591		5029
ACHE	-0.63	5.10	12.91	3.26E-04	4.23E-02	ENSG00000087085		43
HSF1	-0.34	5.32	12.88	3.33E-04	4.23E-02	ENSG00000185122		3297
CLUH	-0.39	5.78	12.87	3.34E-04	4.23E-02	ENSG00000132361		23277
GPC1	-0.44	5.43	12.85	3.37E-04	4.23E-02	ENSG00000063660		2817
RBM38	-0.48	6.15	12.81	3.45E-04	4.29E-02	ENSG00000132819		55544
RXRA	-0.35	6.40	12.79	3.49E-04	4.30E-02	ENSG00000186350		6256
RRAD	-0.72	5.67	12.69	3.67E-04	4.47E-02	ENSG00000166592		6236
C11orf89	-0.57	2.87	12.63	3.80E-04	4.50E-02	ENSG00000184682	NA	
ADRM1	-0.37	5.14	12.63	3.80E-04	4.50E-02	ENSG00000130706		11047
PDGFA	-0.39	3.14	12.47	4.14E-04	4.70E-02	ENSG00000197461		5154
SEMA6C	-0.34	6.86	12.46	4.15E-04	4.70E-02	ENSG00000143434		10500
EPN1	-0.37	4.34	12.40	4.30E-04	4.70E-02	ENSG00000063245		29924
SH2B2	-0.53	1.90	12.38	4.34E-04	4.70E-02	ENSG00000160999		10603
PLEKHO1	-0.29	4.27	12.38	4.35E-04	4.70E-02	ENSG00000023902		51177
UPB1	-0.61	0.33	12.36	4.40E-04	4.70E-02	ENSG00000100024		51733
MACROD1	-0.40	6.20	12.35	4.41E-04	4.70E-02	ENSG00000133315		28992

Table S3C. Upregulated gene transcripts in subcutaneous adipose tissue after sleep loss compared with normal sleep.

Gene name	log fc	log cpm	LR	P-value	FDR	Ensembl gene id	Entrez id
ADRB1	0.91	3.85	37.55	8.90E-10	1.25E-05	ENSG00000043591	153
GLYCTK	0.36	4.92	27.53	1.54E-07	5.44E-04	ENSG00000168237	132158
SYTL3	0.39	4.13	24.86	6.16E-07	9.97E-04	ENSG00000164674	94120
NET1	0.64	7.82	24.86	6.16E-07	9.97E-04	ENSG00000173848	10276
ATP10A	0.31	4.81	23.56	1.21E-06	1.40E-03	ENSG00000206190	57194
RGS3	0.66	7.00	23.35	1.35E-06	1.40E-03	ENSG00000138835	5998
C5orf30	1.15	5.31	23.30	1.39E-06	1.40E-03	ENSG00000181751	90355
NOD1	0.39	5.55	23.06	1.57E-06	1.47E-03	ENSG00000106100	10392
VEGFA	0.44	8.09	22.07	2.63E-06	2.24E-03	ENSG00000112715	7422
ARHGAP24	0.29	6.25	21.28	3.96E-06	2.79E-03	ENSG00000138639	83478
PPP2R1B	0.37	8.80	20.08	7.42E-06	4.63E-03	ENSG00000137713	5519
IL1RAP	0.60	3.86	20.05	7.56E-06	4.63E-03	ENSG00000196083	3556
SLC19A3	0.36	9.19	19.96	7.91E-06	4.65E-03	ENSG00000135917	80704
ID4	0.53	5.08	19.75	8.82E-06	4.97E-03	ENSG00000172201	3400
LRRN3	0.58	4.34	19.16	1.20E-05	6.06E-03	ENSG00000173114	54674
MAP3K8	0.51	4.70	18.53	1.67E-05	7.59E-03	ENSG00000107968	1326
C10orf10	0.75	9.03	18.41	1.78E-05	7.84E-03	ENSG00000165507	11067
LUZP2	0.53	3.49	18.32	1.86E-05	7.96E-03	ENSG00000187398	338645
HTRA3	0.35	6.06	18.08	2.11E-05	8.51E-03	ENSG00000170801	94031
PTGER4	0.33	4.17	17.99	2.22E-05	8.70E-03	ENSG00000171522	5734
RPH3AL	0.28	4.01	17.49	2.89E-05	1.04E-02	ENSG00000181031	9501
FOSL2	0.38	6.92	17.44	2.96E-05	1.04E-02	ENSG00000075426	2355
ZFAND5	0.44	8.74	17.26	3.27E-05	1.12E-02	ENSG00000107372	7763
GRHL1	0.85	2.93	17.22	3.32E-05	1.12E-02	ENSG00000134317	29841
THBS2	0.32	5.76	17.03	3.68E-05	1.18E-02	ENSG00000186340	7058
ENG	0.31	6.22	16.66	4.47E-05	1.37E-02	ENSG00000106991	2022
MOCS1	0.21	7.44	16.62	4.58E-05	1.37E-02	ENSG00000124615	4337
NDUFS7	0.29	4.85	16.23	5.60E-05	1.61E-02	ENSG00000115286	374291
PHLPP1	0.25	5.93	16.00	6.34E-05	1.79E-02	ENSG00000081913	23239
ADAMTS16	0.44	2.36	15.69	7.45E-05	2.06E-02	ENSG00000145536	170690

MAP3K13	0.46	4.86	15.24	9.46E-05	2.42E-02	ENSG00000073803	9175
TWIST1	0.24	5.52	15.17	9.80E-05	2.47E-02	ENSG00000122691	7291
TLR4	0.24	6.92	15.05	1.05E-04	2.54E-02	ENSG00000136869	7099
DDR1	0.40	5.35	14.72	1.25E-04	2.98E-02	ENSG00000204580	780
RARB	0.53	2.30	14.55	1.37E-04	3.10E-02	ENSG00000077092	5915
GPCPD1	0.25	7.03	14.43	1.45E-04	3.19E-02	ENSG00000125772	56261
ISM1	0.45	2.42	14.41	1.47E-04	3.19E-02	ENSG00000101230	140862
ABCA2	0.25	6.14	14.41	1.47E-04	3.19E-02	ENSG00000107331	20
ARHGEF26	0.37	5.50	14.32	1.54E-04	3.25E-02	ENSG00000114790	26084
ARL4D	0.48	1.86	14.29	1.57E-04	3.25E-02	ENSG00000175906	379
SPON2	0.29	4.52	14.21	1.64E-04	3.35E-02	ENSG00000159674	10417
THBD	0.42	3.53	14.13	1.70E-04	3.40E-02	ENSG00000178726	7056
STAB1	0.29	7.73	14.12	1.71E-04	3.40E-02	ENSG00000010327	23166
KIF26A	0.29	4.28	13.96	1.87E-04	3.55E-02	ENSG00000066735	26153
ARHGEF3	0.45	5.11	13.92	1.90E-04	3.55E-02	ENSG00000163947	50650
TM7SF2	0.27	6.47	13.74	2.10E-04	3.76E-02	ENSG00000149809	7108
FBLN2	0.23	9.11	13.73	2.11E-04	3.76E-02	ENSG00000163520	2199
TP53I3	0.31	3.95	13.51	2.38E-04	4.08E-02	ENSG00000115129	9540
RDH5	0.26	5.98	13.41	2.50E-04	4.25E-02	ENSG00000135437	5959
FBXW5	0.22	6.26	13.35	2.59E-04	4.34E-02	ENSG00000159069	54461
C8orf4	0.32	4.20	13.24	2.74E-04	4.49E-02	ENSG00000176907	56892
RDH10	0.39	5.77	13.24	2.75E-04	4.49E-02	ENSG00000121039	157506
CD14	0.35	5.10	13.22	2.77E-04	4.49E-02	ENSG00000170458	929
TIMM13	0.21	4.48	13.19	2.82E-04	4.51E-02	ENSG00000099800	26517
GPBAR1	0.47	2.47	13.06	3.02E-04	4.71E-02	ENSG00000179921	151306
KLHDC7A	0.74	1.86	13.01	3.10E-04	4.75E-02	ENSG00000179023	127707
ABHD5	0.30	6.66	12.89	3.30E-04	4.97E-02	ENSG00000011198	51099
MYEOV	0.50	1.97	12.88	3.31E-04	4.97E-02	ENSG00000172927	26579
GPX1	0.26	7.57	12.82	3.43E-04	4.98E-02	ENSG00000233276	2876
F3	0.42	6.58	12.82	3.43E-04	4.98E-02	ENSG00000117525	2152

Table S3D. Downregulated gene transcripts in subcutaneous adipose tissue after sleep loss compared with normal sleep.

Gene name	Log fc	Log cpm	LR	P-value	Q-value	Ensembl gene id	Entrez id
LONRF1	-0.46	6.69	34.40	4.49E-09	3.17E-05	ENSG00000154359	91694
DES	-1.61	2.08	28.93	7.51E-08	3.53E-04	ENSG00000175084	1674
CPEB4	-0.25	6.87	25.76	3.86E-07	9.97E-04	ENSG00000113742	80315
SIX1	-0.59	6.09	24.66	6.84E-07	9.97E-04	ENSG00000126778	6495
SIX4	-0.48	4.00	24.65	6.89E-07	9.97E-04	ENSG00000100625	51804
MAGI1	-0.31	7.59	24.60	7.07E-07	9.97E-04	ENSG00000151276	9223
NHS	-0.34	5.13	23.55	1.22E-06	1.40E-03	ENSG00000188158	4810
AXIN2	-0.86	4.10	21.97	2.77E-06	2.24E-03	ENSG00000168646	8313
FHOD3	-0.47	4.25	21.90	2.87E-06	2.24E-03	ENSG00000134775	80206
LARGE	-0.33	5.65	21.30	3.93E-06	2.79E-03	ENSG00000133424	9215
PCF11	-0.22	7.12	20.67	5.44E-06	3.65E-03	ENSG00000165494	51585
C12orf23	-0.26	5.35	19.23	1.16E-05	6.06E-03	ENSG00000151135	90488
CCL14	-0.59	3.35	19.18	1.19E-05	6.06E-03	ENSG00000213494	6358
FSTL3	-0.41	5.69	18.88	1.39E-05	6.62E-03	ENSG00000070404	10272
RASD1	-0.76	7.07	18.86	1.41E-05	6.62E-03	ENSG00000108551	51655
BCL6	-0.26	8.06	18.23	1.96E-05	8.11E-03	ENSG00000113916	604
JPH2	-0.77	2.17	17.92	2.30E-05	8.77E-03	ENSG00000149596	57158
CLTCL1	-0.28	5.03	17.63	2.68E-05	9.95E-03	ENSG00000070371	8218
SLC38A2	-0.29	7.89	17.15	3.45E-05	1.13E-02	ENSG00000134294	54407
HILPDA	-0.61	6.42	16.69	4.40E-05	1.37E-02	ENSG00000135245	29923
ARFGAP3	-0.18	5.47	16.38	5.17E-05	1.52E-02	ENSG00000242247	26286
BHMT	-0.72	0.66	15.58	7.93E-05	2.15E-02	ENSG00000145692	635
KCNK2	-0.73	1.06	15.50	8.26E-05	2.20E-02	ENSG00000082482	3776
ENOX1	-0.39	4.06	15.31	9.14E-05	2.39E-02	ENSG00000120658	55068
PTBP2	-0.22	6.00	15.14	9.99E-05	2.47E-02	ENSG00000117569	58155
ESR1	-0.33	5.63	14.67	1.28E-04	2.98E-02	ENSG00000091831	2099
TSKU	-0.52	7.50	14.66	1.29E-04	2.98E-02	ENSG00000182704	25987
MYBPC1	-1.12	1.99	14.31	1.55E-04	3.25E-02	ENSG00000196091	4604
TIPARP	-0.23	5.58	14.08	1.75E-04	3.42E-02	ENSG00000163659	25976
IP6K3	-1.35	-0.05	14.00	1.83E-04	3.53E-02	ENSG00000161896	117283

DDIT3	-0.33	4.85	13.91	1.91E-04	3.55E-02	ENSG00000175197	1649
TOB2	-0.33	7.16	13.82	2.01E-04	3.67E-02	ENSG00000183864	10766
TMEM100	-0.36	5.55	13.65	2.20E-04	3.87E-02	ENSG00000166292	55273
ARID3A	-0.31	4.66	13.53	2.35E-04	4.08E-02	ENSG00000116017	1820
MYH7	-1.07	2.17	13.10	2.95E-04	4.67E-02	ENSG00000092054	4625
ITPKC	-0.23	5.44	13.05	3.04E-04	4.71E-02	ENSG00000086544	80271
ZNF395	-0.18	6.01	12.85	3.38E-04	4.98E-02	ENSG00000186918	55893

Table S4. Altered pathways and transcription factors based on RNA-seq data from skeletal muscle and subcutaneous adipose tissue in response to acute sleep loss compared with normal sleep. (**A-D**) Lists KEGG pathways that are enriched based on gene set enrichment analysis (GSEA) of mRNA transcripts that were (**A**) upregulated or (**B**) downregulated in skeletal muscle, as well as (**C**) upregulated or (**D**) downregulated in subcutaneous adipose tissue after sleep loss compared with after sleep. Also listed are: the mean statistical value (Stat mean), adjusted P-value (q value) and set size of a given pathway, *i.e.* the number of genes included in the gene set test. (**E-F**) *In silico* ChIP enrichment analysis in skeletal muscle and subcutaneous adipose tissue in response to acute sleep loss. Analysis done against the ChEA database (*63*), based on genes upregulated in (**E**) skeletal muscle or (**F**) subcutaneous adipose tissue in response to sleep loss compared with sleep. Showing pathways with adjusted P-value (q-value, FDR) below 0.05; also displaying information on the experiment on which the information is based and the overlap of target genes for a given transcription factor; as well as Z-scores and the significant differentially expressed genes for each tissue that contribute to the overlap.

Table S4A. Upregulated KEGG pathways in skeletal muscle based on RNA-seq in response to acute sleep loss compared with normal sleep.

Pathway	Stat mean	q-value	Set size
hsa04610 Complement and coagulation cascades	0.46	0.00001	39
hsa04520 Adherens junction	0.32	0.00015	62
hsa04512 ECM-receptor interaction	0.31	0.00015	66
hsa04810 Regulation of actin cytoskeleton	0.18	0.0011	167
hsa04666 Fc gamma R-mediated phagocytosis	0.24	0.0045	80
hsa04510 Focal adhesion	0.15	0.011	176
hsa04630 Jak-STAT signaling pathway	0.2	0.018	88
hsa04110 Cell cycle	0.19	0.024	93
hsa00140 Steroid hormone biosynthesis	0.46	0.041	14
hsa04974 Protein digestion and absorption	0.25	0.043	45
hsa04670 Leukocyte transendothelial migration	0.19	0.043	84

Table S4B. Downregulated KEGG pathways based on RNA-seq in skeletal muscle in response to acute sleep loss compared with normal sleep.

Pathway	Stat mean	q-value	Set size
hsa03010 Ribosome	0.58	0.00E+00	85
hsa00190 Oxidative phosphorylation	0.39	0.00E+00	117
hsa03050 Proteasome	0.46	1.40E-06	41

hsa04260 Cardiac muscle contraction	0.33	4.00E-05	62
hsa03040 Spliceosome	0.23	6.80E-05	123
hsa03013 RNA transport	0.18	5.00E-03	136
hsa03410 Base excision repair	0.32	4.50E-02	31

Table S4C. Upregulated KEGG pathways based on RNA-seq in subcutaneous adipose tissue in response to acute sleep loss compared with normal sleep.

Pathway	**Stat mean**	**q-value**	**Set size**
hsa00190 Oxidative phosphorylation	0.41	0.00E+00	119
hsa03010 Ribosome	0.31	9.20E-06	84
hsa00280 Valine, leucine and isoleucine degradation	0.42	2.10E-05	41
hsa00620 Pyruvate metabolism	0.36	4.30E-03	34
hsa04380 Osteoclast differentiation	0.2	4.30E-03	114
hsa00640 Propanoate metabolism	0.38	4.30E-03	30
hsa00020 Citrate cycle (TCA cycle)	0.39	4.80E-03	28
hsa00360 Phenylalanine metabolism	0.64	4.80E-03	10
hsa04145 Phagosome	0.18	4.80E-03	124
hsa00380 Tryptophan metabolism	0.37	4.80E-03	30
hsa04260 Cardiac muscle contraction	0.27	4.80E-03	54
hsa04610 Complement and coagulation cascades	0.3	4.80E-03	45
hsa04620 Toll-like receptor signaling pathway	0.22	4.80E-03	81
hsa00071 Fatty acid metabolism	0.32	6.50E-03	36
hsa04630 Jak-STAT signaling pathway	0.19	9.50E-03	97
hsa00630 Glyoxylate and dicarboxylate metabolism	0.46	1.00E-02	16
hsa01040 Biosynthesis of unsaturated fatty acids	0.41	1.10E-02	20
hsa04122 Sulfur relay system	0.56	1.60E-02	10

hsa00410 beta-Alanine metabolism	0.41	1.70E-02	18
hsa00010 Glycolysis / Gluconeogenesis	0.25	2.00E-02	46
hsa00030 Pentose phosphate pathway	0.36	2.90E-02	21
hsa04975 Fat digestion and absorption	0.33	4.00E-02	24
hsa00830 Retinol metabolism	0.35	4.60E-02	21

Table S4D. Downregulated KEGG pathways based on RNA-seq in subcutaneous adipose tissue in response to acute sleep loss compared with normal sleep.

Pathway	**Stat mean**	**q-value**	**Set size**
hsa03040 Spliceosome	0.23	0.00026	124
hsa03013 RNA transport	0.21	0.00026	139
hsa03050 Proteasome	0.31	0.024	41

Table S4E. ChIP Enrichment Analysis based on genes *upregulated* in skeletal muscle in response to sleep loss**.**

Term	Overlap	Q-value	Z-score	Combined Score	Genes
PPARG_20176806_ChIP-Seq_3T3-L1_Mouse	9/1807	0.01221	-1.59128	16.78399	KANK1; CPT1A; NNMT; PFKFB3; PPP2R1B; FZD5; PDK4; TXNIP; TMEM154
LXR_22158963_ChIP-Seq_LIVER_Mouse	9/2000	0.01375	-1.42086	13.83293	USP6NL; CPT1A; NNMT; PFKFB3; PPP2R1B; FZD5; PDK4; TXNIP; TMEM154

Table S4F. ChIP Enrichment Analysis based on genes *upregulated* in subcutaneous adipose tissue in response to sleep loss.

Term	Overlap	Q-value	Z-score	Combined Score	Genes
SMC1_22415368_ChIP-Seq_MEFs_Mouse	19/2000	0.00197	-1.49300	18.82215	DDR1; ABCA2; SPON2; RPH3AL; PHLPP1; LRRN3; HTRA3; TWIST1; NOD1; F3; FOSL2; ADAMTS16; THBD; NDUFS7; KIF26A; RDH10; RARB; RDH5; MAP3K8
CEBPD_21427703_ChIP-Seq_3T3-L1_Mouse	16/1735	0.01063	-1.58170	16.17996	HTRA3; ZFAND5; TWIST1; ATP10A; IL1RAP; ABHD5; ISM1; THBS2; SYTL3; ARHGAP24; VEGFA; FOSL2; ADAMTS16; ARL4D; THBD; RDH10
FOXA1_25552417_ChIP-Seq_VCAP_Human	17/2000	0.01071	-1.48179	14.54640	DDR1; PTGER4; RPH3AL; GLYCTK; TIMM13; C8ORF4; NOD1; ADRB1; GRHL1; GPCPD1; FOSL2; TM7SF2; THBD; ID4; RARB; MAP3K13; C5ORF30
RELA_24523406_ChIP-Seq_FIBROSARCOMA_Human	12/1182	0.02311	-1.71996	14.91658	DDR1; PTGER4; RPH3AL; TP53I3; KIF26A; TWIST1; RDH5; MAP3K8; THBS2; F3; FOSL2; ENG
TCF21_26020271_ChIP-Seq_SMOOTH_MUSCLE_Human	16/2000	0.02311	-1.55391	13.26517	PTGER4; HTRA3; MYEOV; C10ORF10; TIMM13; GPBAR1; FBLN2; SYTL3; VEGFA; FOSL2; ADAMTS16; THBD; RGS3; ID4; RDH5; MAP3K8
WDR5_24793694_ChIP-Seq_LNCAP_Human	9/757	0.03502	-2.48331	19.43986	PTGER4; NDUFS7; PPP2R1B; RDH10; TIMM13; ABHD5; FOSL2; ENG; TM7SF2

SUZ12_20075857_ChIP-Seq_MESCs_Mouse	25/4356	0.03502	-0.87692	6.82635	DDR1; PTGER4; PHLPP1; LUZP2; HTRA3; TWIST1; ATP10A; NOD1; ADRB1; IL1RAP; ABHD5; ISM1; ADAMTS16; THBD; RDH10; MAP3K8; CD14; ABCA2; RPH3AL; F3; ARHGAP24; FOSL2; KIF26A; ID4; RARB
SMAD3_21741376_ChIP-Seq_ESCs_Human	15/2000	0.04798	-1.59917	11.73154	DDR1; RPH3AL; MYEOV; TIMM13; KLHDC7A; ABHD5; ISM1; VEGFA; FOSL2; ADAMTS16; NDUFS7; ID4; RARB; MOCS1; TLR4

Table S5. Enriched pathways based on proteomic analyses of skeletal muscle tissue in response to acute sleep loss compared with normal sleep. Lists KEGG pathways that are enriched based on mass spectrometry-based proteomic identification of proteins that were significantly (**A**) upregulated or (**B**) downregulated (in their abundance) in skeletal muscle, after sleep loss compared with after sleep. Listing the KEGG pathways, the total number of elements in each pathway ("N"), the number of proteins of a given pathway that were differentially expressed ("DE"), and the FDR-adjusted p value (q value) for the pathway in response to sleep loss. See also Fig. 3 in main text.

Table S5A. Enriched KEGG pathways based on proteins with *increased* abundance in skeletal muscle after sleep loss compared with after sleep

KEGG pathway	N	DE	q value
Cysteine and methionine metabolism	10	2	1.89E-03
Apoptosis - multiple species	2	1	1.43E-02
Sulfur metabolism	2	1	1.43E-02
Sulfur relay system	2	1	1.43E-02
IL-17 signaling pathway	3	1	2.14E-02
p53 signaling pathway	3	1	2.14E-02
Th17 cell differentiation	4	1	2.85E-02
Pathways in cancer	48	2	4.19E-02
Progesterone-mediated oocyte maturation	7	1	4.94E-02

Table S5B. Enriched KEGG pathways based on proteins with *decreased* abundance in skeletal muscle after sleep loss compared with after sleep

KEGG pathway	N	DE	q value
Glycolysis / Gluconeogenesis	32	6	2.78E-06
Fructose and mannose metabolism	8	3	1.58E-04
Pentose phosphate pathway	11	3	4.54E-04
Biosynthesis of amino acids	30	4	7.76E-04
Central carbon metabolism in cancer	14	3	9.75E-04
Carbon metabolism	64	5	1.80E-03
Parathyroid hormone synthesis, secretion and action	5	2	2.18E-03
HIF-1 signaling pathway	20	3	2.89E-03
Glucagon signaling pathway	30	3	9.40E-03
Wnt signaling pathway	13	2	1.59E-02
Chemokine signaling pathway	14	2	1.83E-02
AMPK signaling pathway	16	2	2.38E-02
Tight junction	45	3	2.86E-02

Hedgehog signaling pathway	2	1	3.09E-02
Taste transduction	2	1	3.09E-02
Type II diabetes mellitus	2	1	3.09E-02
Purine metabolism	19	2	3.30E-02
Ras signaling pathway	21	2	3.98E-02
Vascular smooth muscle contraction	21	2	3.98E-02
Pyruvate metabolism	22	2	4.34E-02
Cocaine addiction	3	1	4.60E-02
Cortisol synthesis and secretion	3	1	4.60E-02

Table S6. Changes in serum, skeletal muscle, and subcutaneous adipose tissue metabolites in response to acute sleep loss. (**A**) Analysis of variance (ANOVA) results, and (**B**) log_2 fold changes for *serum* metabolites identified by gas chromatography-based mass spectrometry (GCMS). The analysis is based on a comparison of metabolite levels in samples after sleep loss compared with values obtained after normal sleep (*Wake* effect), for baseline vs. post-oral glucose tolerance (OGTT) values (*Time* effect in (**A**)). Log_2 fold changes comparing sleep loss with sleep (wake:sleep) in (**B**-**D**) are shown as mean ± S.E.M across the analyzed subjects, and were analyzed with two-sided t-tests. Only significant values or statistical trends are shown: significant values ($P<0.05$) are shown in italic bold font; trends ($0.05<P<0.10$) in bold font. Names of metabolites with significant or statistical trends for main effects of *Wake* have been indicated in italic bold or bold, respectively, whereas blank fields indicate metabolites with $P>0.10$. n=15 pairs for all analyses. (**C**) Changes in metabolites identified by GCMS, in response to acute sleep loss, was also investigated in skeletal muscle (n=13 pairs) and (**D**) subcutaneous adipose tissue d, from vastus lateralis muscle and subcutaneous adipose tissue biopsy samples, respectively, obtained in the fasting state after both sleep loss and after normal sleep.

Table S6A. ANOVA results for *serum* metabolites analyzed in the fasting and post-OGTT state after sleep loss and after normal sleep.

Metabolite name	***Wake* effect**	***Time* effect**	**Interaction (*Wake**Time*) effect**
1-palmitoyl-sn-glycero-3-phosphocholine		***0.023***	
1,5-anhydro-d-glucitol	***0.028***	***0.006***	
2-aminobutyric acid			
2-oxoisocaproic acid	**0.096**	***0.000***	
3-hydroxybutyric acid	**0.097**	***0.000***	***0.046***
Adenosine			
Alanine			
Alpha-tocopherol		***0.005***	
Arabitol			**0.091**
Campesterol			
Citric acid		***0.000***	
Creatinine	***0.002***		
Cysteine		***0.001***	
Cystine		***0.001***	
Docosahexaenoic acid		***0.000***	
Dodecanoic acid		***0.000***	**0.078**
Eicosapentaenoic acid		***0.000***	
Eicosatetraenoic acid		***0.000***	***0.044***
Erythritol		***0.005***	
Fructose		***0.002***	
Fumaric acid		***0.004***	
Glucose		***0.001***	***0.046***

Glutamic acid		***0.013***	
Glutamine	***0.028***	***0.008***	
Glycerol-2-phosphate			
Glycerol-3-phosphate		***0.023***	
Glycine		***0.011***	
Heptadecanoic acid		***0.000***	
Hexadecanoic acid		***0.000***	
Inosine			
Inositol		***0.001***	
Isoleucine		***0.000***	
Lactic acid		***0.001***	
Lysine	**0.089**	***0.010***	
Malic acid		**0.099**	**0.098**
Myristoleic acid		***0.000***	
Octadecadienoic acid		***0.000***	
Octadecanoic acid		***0.000***	***0.045***
Octadecenoic acid		***0.000***	**0.071**
Phenylalanine	**0.098**	***0.000***	***0.043***
Pyroglutamic acid		***0.000***	
Serine		***0.000***	
Tryptophan		***0.003***	
Tyrosine	**0.099**	***0.000***	***0.004***
Urea	***0.005***	***0.001***	
Uric acid		***0.001***	
Valine		***0.000***	

Table S6B. Changes in *serum* metabolites in the fasting and post-OGTT state after sleep loss (wake) compared with after sleep.

	Baseline (fasting) differences			**Post-OGTT differences**		
Compound name	**Log_2 ratio (wake:sleep)**	S.E.M.	P-value	**Log_2 ratio (wake:sleep)**	S.E.M.	P-value
1-palmitoyl-sn-glycero-3-phosphocholine	-0.01	0.06		-0.01	0.08	
1,5-anhydro-d-glucitol	***-0.06***	***0.02***	***0.013***	**-0.05**	**0.03**	**0.095**
2-aminobutyric acid	0.00	0.20		-0.30	0.24	
2-oxoisocaproic acid	***0.14***	***0.06***	***0.021***	0.06	0.07	
3-hydroxybutyric acid	**0.83**	**0.39**	**0.054**	0.07	0.18	
Adenosine	-0.15	0.30		-0.23	0.18	
Alanine	-0.17	0.19		0.03	0.22	
Alpha-tocopherol	-0.05	0.11		0.04	0.04	

Arabitol	-0.02	0.06		**0.11**	**0.06**	**0.091**
Arginine	***-0.15***	***0.06***	***0.029***	-0.10	0.07	
Asparagine	***-0.18***	***0.04***	***0.001***	-0.06	0.07	
Campesterol	0.10	0.18		-0.03	0.15	
Citric acid	-0.04	0.08		-0.15	0.11	
Creatinine	-0.15	0.10		***-0.30***	***0.07***	***<0.001***
Cysteine	-0.01	0.06		-0.05	0.07	
Cystine	-0.04	0.10		0.07	0.04	
Docosahexaenoic acid	-0.03	0.09		-0.17	0.10	
Dodecanoic acid	0.13	0.15		-0.19	0.12	
Eicosapentaenoic acid	0.05	0.06		-0.01	0.06	
Eicosatetraenoic acid	0.04	0.05		-0.11	0.06	
Erythritol	-0.02	0.02		-0.05	0.05	
Fructose	-0.29	0.21		0.03	0.18	
Fumaric acid	0.06	0.14		0.13	0.16	
Glucose	-0.05	0.03		**0.05**	**0.03**	**0.069**
Glutamic acid	0.04	0.08		0.16	0.12	
Glutamine	**-0.45**	**0.21**	**0.051**	-0.34	0.22	
Glycerol-2-phosphate	-0.01	0.06		-0.02	0.11	
Glycerol-3-phosphate	-0.06	0.05		-0.07	0.08	
Glycine	-0.13	0.10		-0.06	0.07	
Heptadecanoic acid	0.08	0.11		-0.05	0.11	
Hexadecanoic acid	0.10	0.08		-0.01	0.05	
Inosine	-0.01	0.19		-0.10	0.14	
Inositol	0.00	0.04		0.03	0.05	
Isoleucine	-0.01	0.07		0.00	0.07	
Lactic acid	0.09	0.07		0.04	0.12	
Lysine	-0.37	0.28		-0.50	0.31	
Malic acid	0.17	0.11		-0.02	0.06	
Myristoleic acid	0.17	0.17		-0.17	0.25	
Octadecadienoic acid	0.11	0.10		-0.03	0.09	
Octadecanoic acid	**0.10**	**0.06**	**0.081**	-0.05	0.05	
Octadecenoic acid	0.18	0.14		-0.14	0.17	
Ornithine	***-0.14***	***0.05***	***0.017***	-0.07	0.06	
Phenylalanine	0.01	0.04		***0.13***	***0.06***	***0.040***
Pyroglutamic acid	0.01	0.04		0.02	0.02	

Serine	-0.08	0.05		-0.01	0.07	
Threonine	***-0.19***	***0.07***	***0.015***	***-0.14***	***0.05***	***0.019***
Tryptophan	0.00	0.04		0.04	0.04	
Tyrosine	0.00	0.13		***-0.51***	***0.19***	***0.019***
Urea	***-0.33***	***0.11***	***0.012***	***-0.41***	***0.17***	***0.032***
Uric acid	-0.03	0.06		**-0.07**	**0.03**	**0.064**
Valine	-0.03	0.055		0.00	0.04	

Table S6C. Changes in *skeletal muscle* metabolites after sleep loss (wake) compared with after sleep.

Compound name	**Log_2 ratio (wake:sleep)**	**S.E.M.**	**P-value**
1,5-anhydroglucitol	-0.06	0.08	
3-hydroxybutyric acid	0.60	0.39	
Adenosine-5-monophosphate	0.24	0.14	
Adenosine	0.01	0.18	
Alanine	-0.05	0.09	
Beta-alanine	-0.16	0.15	
Cholesterol	0.07	0.09	
Citrulline	0.02	0.11	
Creatinine	0.06	0.07	
Fructose-6-phosphate	0.29	0.38	
Fructose	0.15	0.31	
Fumaric acid	**-0.39**	**0.19**	**0.057**
Glucose-6-phosphate	0.52	0.39	
Glucose	0.36	0.26	
Glutamic acid	-0.13	0.17	
Glutamine	-0.41	0.23	
Glutamine	-0.39	0.29	
Glutamine	-0.27	0.20	
Glyceric acid-3-phosphate	-0.10	0.18	
Glycerol-2-phosphate	-0.19	0.18	
Glycerol-3-phosphate	-0.23	0.16	
Glycine	***-0.20***	***0.12***	***0.046***
Glycine	-0.13	0.15	
Heptadecanoic acid	0.03	0.14	
Hexadecanoic acid	**0.17**	**0.08**	**0.065**
Histidine	-0.01	0.14	
Inosine	-0.21	0.49	
Inositol, scyllo	-0.04	0.10	

Isoleucine	0.04	0.10	
Lysine	0.07	0.12	
Malic acid	0.11	0.15	
Octadecanoic acid	0.11	0.08	
Octadecenoic acid	0.24	0.13	
Ornithine	0.06	0.13	
Pantothenic acid	-0.14	0.14	
Phosphate-fragment	0.01	0.05	
Proline	-0.13	0.09	
Pyroglutamic acid	0.03	0.07	
Pyrophosphate	-0.19	0.14	
Serine	-0.09	0.09	
Succinic acid	-0.10	0.08	
Taurine	-0.29	0.20	
Threonine	**-0.16**	**0.09**	**0.051**
Urea	**-0.42**	**0.22**	**0.061**
Uric acid	-0.07	0.30	
Valine	0.02	0.09	

Table S6D. Changes in *subcutaneous adipose tissue* metabolites after sleep loss (wake) compared with after sleep.

Compound name	**Log_2 ratio (wake:sleep)**	**S.E.M.**	**P-value**
1,5-Anhydro-d-glucitol	0.17	0.17	
3-Hydroxybutyric acid	***0.73***	***0.35***	***0.045***
4-Hydroxybenzoic acid	0.44	0.43	
Adenosine-5-monophosphate	0.43	0.54	
Adenosine	0.48	0.29	
Alanine	0.25	0.18	
Asparagine	**0.69**	**0.39**	**0.089**
Aspartic acid	***0.52***	***0.24***	***0.039***
Citric acid	0.38	0.27	
Creatinine	-0.39	0.32	
Dodecanoic acid	0.14	0.08	
Glucose	0.22	0.26	
Glutamic acid	***0.53***	***0.23***	***0.027***
Glutamine	0.42	0.38	
Glyceric acid-3-phosphate	***1.21***	***0.51***	***0.020***
Glycerol-3-phosphate	0.30	0.25	
Glycine	0.20	0.20	
Inositol	0.08	0.13	

Inositol	0.17	0.14	
Isoleucine	0.20	0.22	
Lactic acid	0.21	0.14	
Lysine	0.29	0.26	
Malic acid	***0.42***	***0.15***	***0.010***
Myristic acid	0.08	0.15	
Nonanoic acid	***0.13***	***0.06***	***0.042***
Octadecanoic acid	**0.12**	**0.07**	**0.098**
Octadecenoic acid	-0.28	0.59	
Ornithine	0.31	0.33	
Phosphoric acid	0.10	0.20	
Proline	0.27	0.26	
Pyroglutamic acid	***0.49***	***0.22***	***0.032***
Succinic acid	**0.19**	**0.10**	**0.068**
Threonine	0.13	0.17	
Tyrosine	0.34	0.27	
Valine	0.26	0.22	

Supplementary Methods

DNA extraction and DNA methylation analyses

For genomic DNA extraction from subcutaneous adipose tissue and skeletal muscle samples, the QIAamp DNA Mini Kit was used (Qiagen, Hilden, Germany). Concentration and purity of DNA was determined using NanoDrop (ND-1000, Thermo Fisher, MA, USA) and the Quant-iT™ PicoGreen® dsDNA Assay Kit (Thermo Fisher). The EZ DNA Methylation-Gold™ kit (Zymo Research, Irvine, CA, USA) was used to carry out bisulfite conversion, as detailed in ref. (*64*). The Illumina Infinium Methylation Assay protocol was employed to process around 200 ng of bisulfate-converted DNA (bisulfite treatment results in the conversion of cytosine (C) nucleotides that are unmethylated into uracil/thymine (U/T) nucleotides). Following whole-genome DNA amplification, DNA was enzymatically fragmented, precipitated and resuspended. To hybridize locus-specific oligonucleotide primers on the BeadChip, the DNA was then run overnight at 48° C. Following hybridization to the BeadChips, C or T nucleotides were detected using extension of single-base primers and the Illumina iScan was used to measure C- or T-nucleotide corresponding fluorescence signals. To separate possible batch effects from biological signals, respectively, several technical and biological replicates were included (at least one from each of the two experimental conditions).

GenomeStudio 2009.2 (Illumina) was used for initial preprocessing of the fluorescence data, followed by quality control. This included hierarchical clustering for plotting relationships between samples and identifying outliers, and ensuring that technical replicates clustered together. The $\log_2$ ratio of the methylated probe versus unmethylated probe intensities (the M-value) was used for methylation analyses – a statistically more valid representative analysis of differential methylation levels (*65*).

For the R-based analysis, the package minfi was used (*66*)*:* Probes with a detection p-value over 0.01 were removed from the analysis, as were probes overlapping SNPs and non-specific probes. Quantile normalization was used to adjust for systematic differences between arrays, and ComBat was used to adjust for batch effects. Data from adipose and muscle were processed separately. DMRs were called using DMRcate (v 1.14.0) (*67*), which finds differentially methylated regions (DMRs) using a gaussian kernel, ranking the most differentially methylated regions based on a tunable kernel smoothing, that is unbiased by genomic annotation and local differential change in methylation signal. For DMRcate, a model with coefficients for both subject and sleep condition was used, with following parameters and thresholds: lambda = 1000, C = 2, probe FDR < 0.05 and DMR FDR < 0.05. DMRs were then annotated to the nearest a transcription start site within 5Kbp, based on ENSEMBL genome annotations. Fishers exact test was used to for analyzing enrichment of Gene Ontology and KEGG sets among the genes near DRMs, given a background set of all genes near probes on the 450K array. Gene sets with FDR<0.05 were reported.

RNA extraction, qPCR and RNA-seq workflow

RNA extraction was done using Trizol followed by the Qiagen Universal RNeasy Tissue kit for skeletal muscle and the Qiagen RNeasy Lipid kit for adipose tissue samples. RNA concentration and integrity were determined using NanoDrop, and subsequently by Fragment analyzer (Advanced Analytical Technologies) and TapeStation 2200 (Agilent Technologies) (RQN 7.30 ± 0.12 for adipose tissue RNA; RINe 8.46 ± 0.05 for muscle tissue RNA). The SYBR green and Taqman systems (Applied Biosystems) were employed to measure mRNA gene expression, as described in REFs (*68, 69*). SYBR green primers were designed to span exons using Primer3 (http://bioinfo.ut.ee/primer3/) or NCBI Primer-BLAST (http://www.ncbi.nlm.nih.gov/tools/primer-blast/), and were optimized for each target gene. All samples for qPCR were analyzed in duplicates and the ΔCt method

(*70*) was used to normalize the data against the expression of the most consistently expressed house-keeping genes, PPIA and TBP.

RNA library generation (from 0.5 µg total RNA per sample) was performed using the TruSeq Stranded Total RNA kit (Illumina) according to the manufacturers' protocol (#15031048 rev E). All samples were sequenced with paired-end 50-bp read lengths, using the v4 sequencing chemistry, on an Illumina HiSeq2500.

Transcriptome analysis

The RNA-seq pipeline (NGI, Sweden, https://github.com/ewels/NGI-RNAseq) for basic processing of RNA-seq data, included fastqc and RseQc for quality control; Trimgalore for trimming reads; STAR for read alignment (*71*); Picard for removal of duplicate read (*72*); and featureCounts for counting aligned reads to ENSEMBL genes (*73*). The R package gplots was then used to generate PCA plots, which showed a clear separation between adipose tissue and skeletal muscle samples (data not shown), and a high correlation between samples within each tissue (>97% Pearson correlation; data not shown); however, no clear separation was found within each tissue for our intervention (sleep vs. sleep deprivation; data not shown). The R package EdgeR (v. 3.16.5) was used to perform differential gene expression from the data generated by featureCounts, with a model with coefficients for both subject and sleep condition (*74*). Gene set enrichment analysis was carried out using the R package GAGE (v. 2.24), using Gene Ontology annotations and KEGG pathways (*75*). In addition, Enrichr (*76*) was used to look for significant overlaps between differentially expressed genes and gene sets based on ChIP data from the ChEA database (*63*). For correlational analyses between mRNA and DNA methylation levels, ggplot2 and ggExtra were used and DNA methylation levels were averaged for all probes near each gene included in the analysis.

Label-free quantification of relative protein expression using liquid chromatography and tandem mass spectrometry (LC-MS/MS)

Biopsy aliquots were dissolved in a 20 mM HEPES, 9 M Urea lysis buffer supplemented with complete mini EDTA-free protease inhibitor cocktail (Roche Diagnostics Scandinavia, Stockholm, Sweden) and homogenized using micro pestles. Proteins were extracted by sonication using a probe with a 3-mm tip (10 x 1 sec, amplitude 30%) followed by centrifugation for 10 min at 4 °C. The lipid layer of the subcutaneous adipose tissue samples was removed after the final centrifugation step.

For each sample, the total protein concentration was measured using the Bradford Protein Assay (Bio-Rad, Hercules, California, USA). Aliquots corresponding to 20 µg for muscle samples and 10 µg for adipose samples were taken out for digestion. The proteins were reduced with dithiothreitol (DTT, final concentration 50 mM) and alkylated with iodoacetamide (IAA, final concentration 25 mM). After dilution four times with 50 mM ammonium bicarbonate, trypsin (Promega, Madison, WI, USA) was added in a trypsin:protein ratio of 1:20 and digestion was performed overnight at 37 °C. Thereafter the peptides were desalted using Pierce C18 Spin Columns (Thermo Scientific), dried and resolved in 0.1% formic acid (FA) to a final concentration of 0.1 µg/µL for muscle samples and 0.3µg/µL for adipose samples.

The samples were analyzed using a Q Exactive Plus mass spectrometer (Thermo Fisher Scientific, Bremen, Germany) equipped with a nano electrospray ion source. A volume of 5 µL of dissolved peptides was loaded and peptides were separated by reversed phase liquid chromatography using an EASY-nLC 1000 system (Thermo Fisher Scientific, Bremen, Germany). A setup of pre-column and analytical column was used. The pre-column was a 2 cm EASY-column (1D 100 µm, 5 µm C18) (Thermo Fisher Scientific) while the analytical column was a 10 cm EASY-column (ID 75 µm, 3 µm, C18) (Thermo Fisher Scientific). Peptides were eluted with a 150-min linear gradient from 4% to 100% acetonitrile at 250 nL/min. The mass spectrometer was

operated in positive ionization mode acquiring a survey mass spectrum with resolving power 70000 (full width half maximum) and consecutive high collision dissociation (HCD) fragmentation spectra at a resolution of 17500 of the 10 most abundant ions. The mass spectrometer worked in the data-dependent mode. The acquired MS data (.RAW-files) were processed by MaxQuant (v. 1.5.1.2) (*77*). gplots (R package) was used to generate PCA plots of the processed data, but indicated no clear separation within each tissue for our sleep vs. sleep deprivation intervention (data not shown).

For correlational analyses between mRNA and protein expression levels, gplots and edgeR were used. Identified mRNAs and proteins were first filtered, so that only mRNAs/proteins where both the mRNA and proteins had non-zero measurments were included in the analysis. For each analyzed tissue, data from all 30 samples were then merged. Only mRNA/protein pairs where there was a 1:1 mapping between gene and protein were used.

Pathway analysis of proteomics data was carried out using the R package limma (v. 3.30.13) using KEGG pathway annotations (*78*).

Gas chromatography-mass spectrometry (GCMS) metabolomic analyses

Gas chromatograpy-mass spectrometry (GCMS) was performed as previously described in refs. (*79*) and (*80*). For skeletal muscle and serum samples, extraction buffer (1000 µL; 80/20 v/v methanol:water) with internal standards was added to the tissue sample (9-12 mg). A tungsten bead was added to the sample, which was then shaken in a mixer mill at 30 Hz for 3 min. For GCMS of serum, extraction buffer (900 µL; 90/10 v/v methanol:water) with internal standards was added to sample material (100 µL). A mixer mill was used to shake the sample at 30 Hz for 3 min, and the sample was then left at +4 °C on ice to precipitate proteins. After the above steps for muscle tissue and serum, the sample was centrifuged (+4 °C, 14 000 rpm, 10 min) and 200 µL of the supernatant were transferred to a micro vial, followed by solvent evaporation. For adipose tissue samples, CHCl3:methanol (250 µL of 2/1; v/v) with D4-Cholic Acid, 50 µL of water with 13C9-phenylalanine, and 2 tungsten beads were added to each sample. The samples were shaken at 30 Hz for 3 min followed by removal of the beads. The samples were then left standing at room temperature for 30 min. The samples were centrifuged (14 000 rpm, +4 °C, 3 min) after which 40 µL of the aqueous phase were transferred to Eppendorf tubes. Methanol (160 µL) with D6-salicylic acid was added to the Eppendorf tubes and remaining proteins were precipitated for one hour at -20 °C. Centrifugation followed (14 000 rpm, +4 °C, 10 min), after which 35 µL supernatant were transferred to GC vials. After evaporation of the solvents, the samples were stored in -80 °C until analysis.

Sample derivatization was performed according to refs. (*79*) and (*80*). For serum and muscle, methoxyamine (30 µL at 15 µg/µL in pyridine) was added to the dry sample after which it was shaken vigorously for 10 min. The reaction was then started by keeping the sample at +70 °C for 60 min before proceeding at room temperature for 16 hours. MSTFA (30 µL) was then added, the sample was shaken, and was left to for 1 hour in room temperature; methyl stearate (30 µL at 15 ng/µL, in heptane) was added before analysis. Adipose tissue sample derivatization started with a smaller addition of methoxyamine (5 µL at 15 µg/µL, in pyridine) to the dry sample. The sample was shaken for 10 min prior to 16 hours of incubation at room temperature. After adding MSTFA (5 µL), the sample was again shaken and left to react for 60 min at room temperature. Before analysis, methyl stearate (5 µL at 15 ng/µL, in heptane) was added to the sample.

For the GCMS analysis, 1 µL of derivatized sample was injected in splitless mode via a CTC Combi Pal autosampler (CTC Analytics AG, Switzerland) into an Agilent 6890 gas chromatograph (10 m x 0.18 mm fused silica capillary column, with a chemically bonded 0.18 µm stationary DB 5-MS UI stationary phase from J&W

Scientific). The effluent of the column was introduced into a Pegasus III time-of-flight mass spectrometer GC/TOFMS (Leco Corp., St Joseph, MI, USA).

Following mass spectrometry analysis, non-processed MS files were exported in NetCDF format to MATLAB R2011b, in which custom scripts were used for pre-analytical procedures (including base-line correction, chromatogram alignment, data compression), as described in ref. (*81*).

Biochemical analyses

Insulin sensitivity in the fasted state was calculated using the HOMA-IR method (*82*). OGTT-related insulin sensitivity was calculated using the Matsuda index (*62*). The ANOVA analysis for cortisol was adjusted for significant sphericity deviation with the Greenhouse-Geiser method for Time and Wake*Time effects.